SVERIGES GEOLOGISKA UNDERSÖKNING

SERIE C NR 712 AVHANDLINGAR OCH UPPSATSER ÅRSBOK 69 NR 4

PAVEL M. ADAMEK

GEOLOGY AND MINERALOGY OF THE KOPPARÅSEN URANINITE-SULPHIDE MINERALIZATION, NORRBOTTEN COUNTY, SWEDEN

STOCKHOLM 1975

SVERIGES GEOLOGISKA UNDERSÖKNING

SERIE C NR 712 AVHANDLINGAR OCH UPPSATSER ÅRSBOK 69 NR 4

PAVEL M. ADAMEK

GEOLOGY AND MINERALOGY OF THE KOPPARÅSEN URANINITE-SULPHIDE MINERALIZATION, NORRBOTTEN COUNTY, SWEDEN

STOCKHOLM 1975

ISBN 91-7158-076-X

Textkartorna på s. 6 och 7 är ur sekretessynpunkt godkända för spridning.
Statens lantmäteriverk 1975-02-11 och 1975-02-18.

C. DAVIDSONS BOKTRYCKERI AB, VÄXJÖ 1975

CONTENTS

Abstract 4
I. Introduction 4
1. General geology 4
II. Stratigraphy of the Kuokkel Group 8
1. Introduction 8
2. Formation A, Bed 1—Bed 4 9
2.1. Massive meta-tuff (Bed 1) 9
2.2. Meta-basic lava (Bed 2) 10
2.3. Banded meta-tuffs (Bed 3) 11
2.4. Quartz-biotite schists (Bed 4) 14
2.5. Remarks on a development of Beds 2—4 15
3. Formation A, Bed 5—Bed 7d 15
3.1. Meta-tuffs and associated rocks of Beds 5 and 7d 16
3.1.1. Meta-tuffs 16
3.1.2. Graphite-bearing meta-tuffites 16
3.1.3. Graphite schists 17
3.1.4. Fragment-bearing rocks 17
3.1.5. Meta-chert 18
3.1.6. Meta-marl 20
3.2. Meta-volcaniclastic psephite (Bed 6 and Bed 7c) 20
4. Formation B 24
5. Meta-porphyrite sills 27
6. Formation C 28
III. Ore mineralizations 30
1. Uranium mineralizations 30
1.1. General features of uranium mineralizations 30
1.2. Some comments on the composition of the host rocks 31
1.2.1. Skarn-like mobilisates 34
1.3. Uranium mineralogy 35
2. Non-radioactive ore mineralizations 40
2.1. General features of mineral assemblages 40
2.2. Mineralogy of the non-radioactive ore minerals 41
2.2.1. Intergrowths of other minerals with pyrite, representing proper blastic textures 42
2.2.2. Bornite, chalcopyrite and digenite intergrowths 47
2.2.3. Textures resembling replacement 50
3. Some remarks on the geochemistry of the uranium mineralizations 51
IV. Discussion and conclusions 55
Acknowledgements 59
References 59
Tables 4a, 4b, 4c, 5, 6a, 6b and figure 42 61
Appendix by A. M. Byström-Brusewitz 68

ABSTRACT

The results of detailed geological and mineralogical investigations of uraninite, magnetite and sulphide mineralizations from the Kopparåsen greenstone belt are given. The ore mineralizations, forming strata-bound bodies, occur at different stratigraphic levels of a complex of supracrustal rocks consisting chiefly of basic meta-tuffs and meta-sediments. Banded meta-tuffs, graphite-bearing meta-tuffites, graphite schists and meta-chert appear as the host rocks of the uranium mineralizations. Excellent exposures of the bedrock, and preservation of many original features permitted a detailed lithostratigraphic division of the observed rock sequence and an analysis of the lithostratigraphic position of the ore occurrence and of the environmental factors in their formation. On the basis of microscope studies of mineral intergrowths, the author deduces a pre-metamorphic origin of the uranium mineralizations and ascertains a multiphase mobilisation of uranium generated by the greenschist-grade metamorphism and subsequent endogenous processes. These conclusions are confirmed, at least to a certain degree, through geochemical investigations. According to the author's interpretation, the uraninite, magnetite and sulphide mineralizations are of a volcanic-sedimentary origin.

I. INTRODUCTION

The Kopparåsen area is one of the districts in northern Sweden which for a long time has attracted the attention of prospectors. Copper and zinc mineralizations were discovered there in 1897 and intensively investigated during the following twenty years. To-day, these mineralizations are only of minor economic interest. In 1963 radioactive anomalies were detected in the area and investigated first by AB Atomenergi and, during the years of 1968—1970, by the Ore Investigations Department of the Geological Survey of Sweden (SGU). A great number of uranium mineralizations were revealed, most of them being associated with the sulphide mineralizations. Excellent outcrops and preservation of many original features of the associated rocks permit a detailed analysis of the lithostratigraphic position of the occurrence and of the environmental factors in its formation. The present report and accompanying maps present geological results of the prospecting work, while the economic ones were published in a separate report (Adamek 1973).

1. GENERAL GEOLOGY

The area dealt with lies within a Precambrian window (the Kuokkel window) in the Scandinavian Caledonides, in the westernmost part of the map sheets 30 I Abisko and 31 I Vadvetjåkka, north of the railway station Kopparåsen. Exposures of the bedrock form more than 70 % of the area, which makes it particularly suitable for geological studies.

The Kuokkel window (Kulling 1964), consists of migmatite granite enclosing relicts of migmatized supracrustal rocks. Only in the central part of the window does a N—S striking belt of well preserved supracrustal rocks occur. This rock sequence, which has been the main target for the uranium prospecting work, will here be called the Kopparåsen greenstone belt. The belt occupies an area which is 9.2 km in length and 1.8 km wide. To the north as well as to the south it is overlain by Coledonian rocks (Fig. 1). Uranium and sulphide mineralizations occur in the eastern and central part of the greenstone belt. The supracrustal rocks are of Precambrian age and have been correlated by Ödman (1957) with rocks of the so called Lapponium. The previous literature concerning the area is sparse. The occurrence of greenstones, which represent the main part of the supracrustal rocks of the area, was reported by Holmquist (1910) who correlated them with the so-called "Sjangeli skiffrar" (Petersson 1897) which occur in another window with Precambrian rocks ca 25 km to the SW. Ödman (l. c.), Tegengren (1924) and Grip, Frietsch (1973) mention the area but provide little further information. Supracrustal rocks have been metamorphosed largely to the greenschist facies, and no primary mineral assemblage are fully preserved. However, relict textures and structures allow the character of the original rocks to be determined. Excellent exposures of the bedrock, with many instructive way-up structures, indicate that the Kopparåsen greenstone belt is built up of a sequence of steeply inclined strata which face west throughout the belt with progressively younger beds when passing from east to west. For these strata, the name Kuokkel Group is here introduced,

The rocks of the Kuokkel Group are intruded by migmatite granite of the so-called Lina type. Contacts between the granite and the rocks of the Kuokkel Group are in general very sharp, in places strongly suggesting an intrusive contact. However, in detail, many features demonstrating a metasomatic replacement of supracrustal rocks are discernible. The rocks of the Kuokkel Group as well as the migmatite granite are cut by basic dykes, one of which can be traced for several kilometres.

During the summers of 1968 and 1969, field investigations furnished the basic information for this paper. Economic aspects led to a certain unevenness in the distribution of the data. Special attention has been given to uranium mineralizations and to the rocks surrounding these mineralizations, while others are described only briefly. The writer spent very little time studying the granite or Caledonian rocks and this paper does not deal with them.

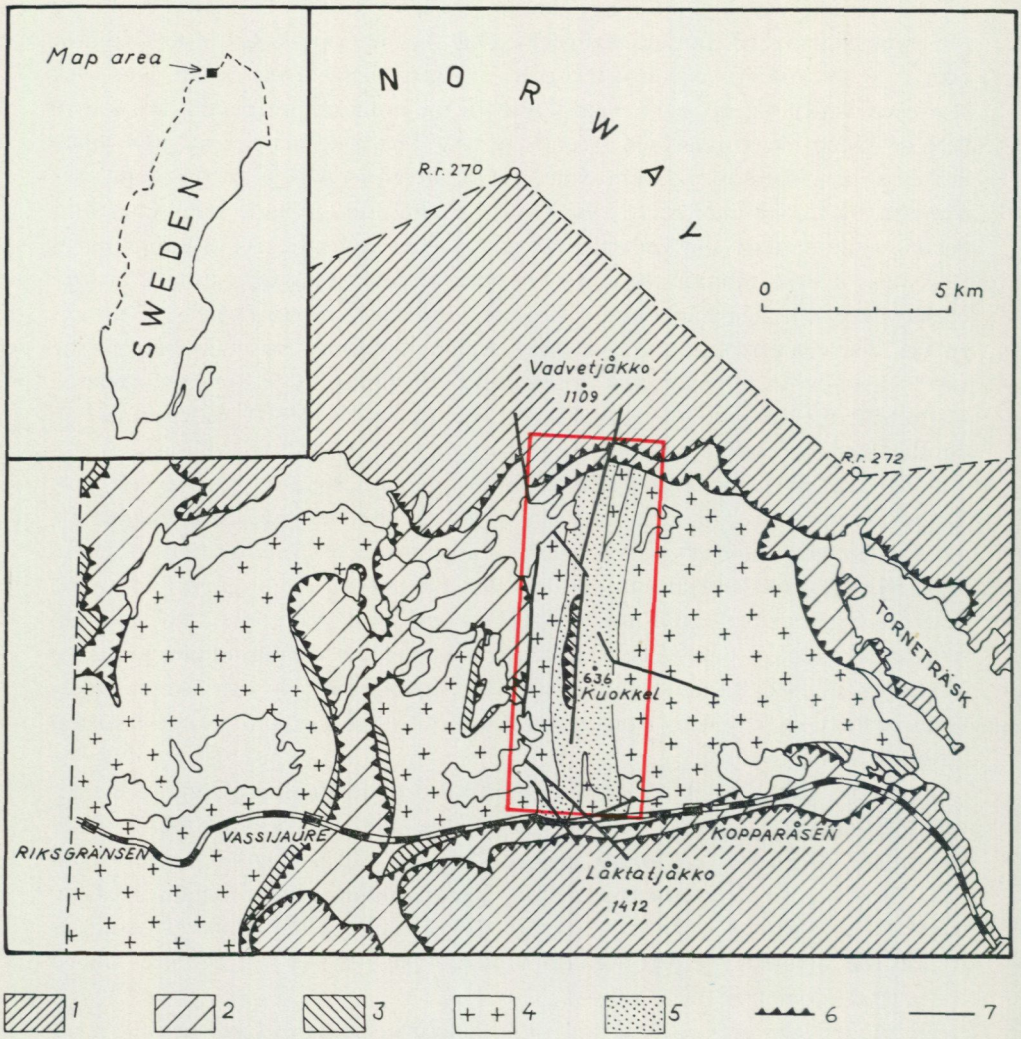

Fig. 1. Geological sketch map of the Kuokkel window. Based mainly on O. Kulling 1964. Legend: 1—3 — Caledonian rocks: 1 — upper nappe complex = Seve-Köli complex; 2 — middle nappe complex; 3 — Torneträsk Group; 4—5 — Precambrian rocks: 4 — migmatite granite; 5 — supracrustal rocks of the Kuokkel Group (Kopparåsen greenstone belt); 6 — thrust; 7 — fault.

The map area shown on Plate 1 is indicated.

Fig. 2. Legend: 1 — Caledonian rocks; 2 — granite; 3 — Kuokkel Group — Formation A; 4 — Kuokkel Group — Formations B and C; 5 — uranium mineralizations connected with Beds 3, 5 and 7d; 6 — magnetite, chalcopyrite and bornite associated with meta-basic lava; 7 — pyrite, pyrrhotite and molybdenite associated with banded meta-tuff; 8 — pyrrhotite, arsenopyrite, pyrite, sphalerite, chalcopyrite and galena associated with meta-tuff, graphitic meta-tuffite, graphite schist and meta-chert; 9 — pyrrhotite, sphalerite, arsenopyrite, pyrite, chalcopyrite, galena, gersdorffite associated with graphitic meta-tuffite interlayered in meta-volcaniclastic rocks and with meta-volcaniclastic psephite itself; 10 — faults.

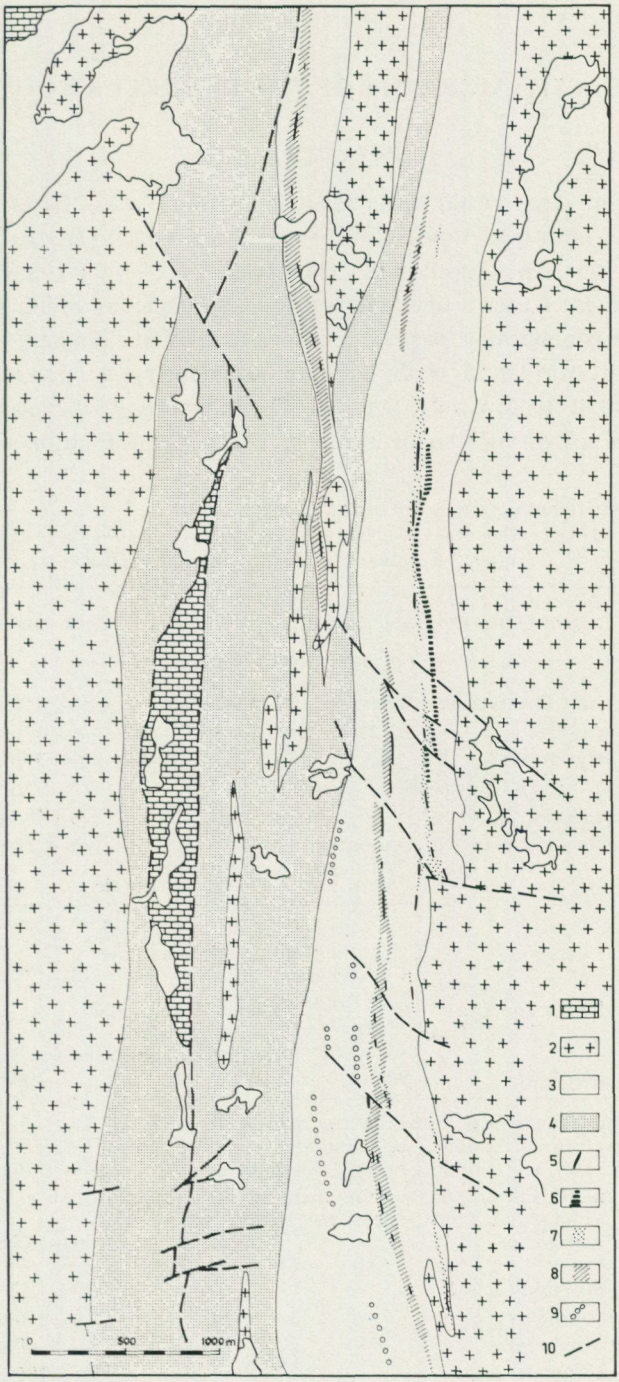

Fig. 2. Sketch map showing the location of ore mineralizations in the Kopparåsen greenstone belt.

II. STRATIGRAPHY OF THE KUOKKEL GROUP

1. INTRODUCTION

The sequence of supracrustal rocks occurring within the Kopparåsen greenstone belt forms one lithostratigraphic unit named the Kuokkel Group. This unit has been divided into three formations. The lower one — Formation A — displays dominant features characteristic of a subaqueous origin in a volcanic environment. Its uppermost part extends as a tongue into the next — Formation B. This formation is dominantly sedimentary containing small-scale features typical of shallow water deposits. The influence of vulcanism is indicated by the occurrence of volcaniclastic rocks. The upper formation — Forma-

TABLE 1. The stratigraphic succession of the Kuokkel Group

		Younger deep-seated rocks (migmatite granite)			
F C	Bed 14	Greenschist (Meta-volcanic turbidite)	180—600 m	Bed 14	F C
		tectonic contact			
FORMATION B	13	Strongly sheared sandstone and pebbly sandstone	30—150 m	13	FORMATION B
	12	Greenschist	0—120 m	12	
	11	Pebbly sandstone	0—370 m	11	
	10	Sandstone and quartzite	15—330 m	10	
	9	Greenschist	0—180 m	9	
	8	Pebbly sandstone and conglomerate	0—250 m	8	
		Conglomerate			
		Meta-tuff with interbeds of graphite schist and meta-chert	0—130 m	7d	FORMATION A
	7b	Sandstone and quartzite 30—210 m		7c	
	7a	Conglomerate 0—90 m	Meta-volcaniclastic psephite (mainly sharpstone conglomerate) 0—200 m		
FORMATION A	6	Meta-volcaniclastic psephite (pyroclastic breccia, lapilli tuff, sharpstone conglomerate) associated with meta-tuff and graphite-bearing meta-tuffite	40—730 m	6	
	5	Meta-tuff and graphite-bearing meta-tuffite with associated graphite schist, meta-cherty tuff, meta-chert and meta-marl	0—155 m	5	
	4	Quartz-biotite schist	0—190 m	4	
	3	Banded meta-tuff	40—230 m	3	
	2	Meta-basic lava	0— 60 m	2	
	1	Massive meta-tuff	100—200 m	1	
		(Basement not known)			

tion C is composed of greenstones representing volcanic turbidites. The contact between Formation B and Formation C is tectonic, consisting of a sizeable shear zone which is the earliest dislocation within the area studied.

The rocks of Formation A and B are intruded by several large porphyrite sills.

Uranium mineralizations and the main part of the sulphide and magnetite mineralizations occur at different levels of Formation A, forming irregular strata-bound bodies.

The stratigraphic succession based on lithology is presented in Table 1. In general, the supracrustal units of the Kopparåsen greenstone belt are similar to those found in the Kiruna (Offerberg 1967), Tärendö (Padget 1970) and Vittangi (Eriksson 1975) areas. However, isolation of the described area does not permit a reliable stratigraphic correlation to be made. Descriptions are given below of the various units.

2. FORMATION A, BED 1—BED 4

Within the mapped area, the lower part of Formation A occupies a zone of varying width west of the contact with granite. It is built up by four beds which consists of

quartz-biotite schist (Bed 4)
banded meta-tuff (Bed 3)
meta-basic lava (Bed 2)
massive meta-tuff* (Bed 1)

Only in the centre of the Kopparåsen greenstone belt does the complete stratigraphic sequence occur. There Bed 1 is overlain by the meta-lava-flow and banded meta-tuff. This tuff passes gradually upwards into quartz-biotite schist. To the south, the lowermost units of the complex, being affected by granite, are not exposed. It is apparent that the quartz-biotite schist pinches out northwards. The top boundary of the whole rock complex (i. e. the contact between Bed 4 and Bed 5) is rather sharp and easily recognized in the exposures.

In the northern part of the area, between the lowermost lithostratigraphic unit and the meta-basic lava or banded meta-tuff overlying it, there are mostly rocks which may best be characterised as "transitional rocks" with varying proportions of massive meta-tuff and banded meta-tuff.

2.1. MASSIVE META-TUFF (BED 1)

The first — lowermost lithostratigraphic unit extending along the eastern granite contact consists of a meta-tuff which is for the most part a very fine-grained, indistinctly bedded, light greenish grey or rusty weathering rock, grey to greenish

* The prefix "meta" is used in this account to designate rocks in which the original fabric can be recognized.

grey on a freshly broken surface. In places the original structureless rock assumes a layered appearance due to quartz-amphibole veinlets which segregated along schistosity planes. Irregular skarnlike veinlets are also common here.

Under the microscope, epidote and amphibole together with olivegreen biotite appear as larger grains with spaces in between occupied by epidote-white mica-albite mass. Quartz, forming as much as 19 % of the rock, partly appears as wedge- and splinter-shaped grains with sharp outlines. No other ore minerals than pyrite occur and pyrite is restricted to one single layer underlying a basic lava (Bed 2).

The massive meta-tuff is the only rock in which effects of a granitization were established with certainty. The meta-tuff is slightly feldspathised in the narrow zone of a few metres close to the granite contact. In the broader zone, the green hornblende is transformed to biotite. Tourmalinization is extensive as well. The tourmaline is developed as bluish brown/beige ragged grains which are gathered into glomeroblastic aggregates, up to 3 mm in diametre. No scapolite was observed in this rock. The granitization seems to be post-metamorphic.

2.2. META-BASIC LAVA (BED 2)

The meta-basic lava is coarse grained. It may contain in places relicts of amygdules and schlieric layers along its contacts, but is in general quite massive and structureless. Consequently, this rock is rather difficult to distinguish from the intrusive sill rocks. The main evidence for distinguishing both rock-types is the presence of lava globes resting on the lava top, which are rarely apparent in the tuffs (Fig. 3). The globes are elongated with originally tough glassy skins, embedded in the altered water-lain tuff. They also appear, quite isolated, about 100 m from the southern edge of the flow, but still in the same stratigraphic horizon. Commonly, where the globes do not occur, the massive lava has a sharp contact with the overlying banded tuffs. Investigations of numerous outcrops in the area studied have not produced any evidence for the existence of more than one lava flow. This flow rests with a sharp contact on the underlying tuffs and attains 60 m thickness in the northern part. Further to the north, it pinches out rapidly. The exposed section of the flow is 2 400 m long.

Similar to other rocks, the lava is fairly recrystallized. Under the microscope the rock is seen to be composed mainly of newly formed minerals. The original plagioclase is replaced by epidote, pale mica, carbonate and albite and the determination of its original composition is impossible. A zonal distribution of magnetite inclusions in some altered grains reflects an original zonal texture of a plagioclase. The amphibole is a bluish green or dusty greyish green, with a low birefrigence. γ/c is 21—24°. It is mostly corroded by epidote. Amphibole of an actinolite type is more rare. Biotite, chlorite and quartz occur only in small amounts. The amount of ore grains (magnetite, bornite, chalcopyrite and others)

Fig. 3. Elongated lava globe resting on the top of a massive lava flow. The globe is surrounded by a water-lain tuff. The contact between Bed 2 and Bed 3. (Compare with the Plate 155 D in Green, Short, 1971.)

varies considerably. As a rule, they are more abundant in the intensively recrystallized parts of the rock enriched in epidote, forming in places layered or schlieren-like bodies. However, all of them are small. Sphene is an accessory. Its typical appearance is in the form of extremely fine-grained aggregates surrounding magnetite grains. Tourmaline and scapolite are rare.

2.3. BANDED META-TUFFS (BED 3)

Bed 3 is one of the uranium-bearing horizons. The meta-tuffs constituting this bed are inhomogeneous rocks of banded structure built up by a set of petrologically different beds. On a weathered surface some beds are light greenish grey or light brownish green with psammitic macrotexture or dense lamination. Other beds, being dark greyish green to blackish green in colour, are for the most part finer grained or massive. The individual beds, which are from a few millimetres to several decimetres thick, commonly show a graded bedding. In places, the light beds change gradually into a cherty type of rock. (Figs. 4 and 5.) A striking feature is the presence of slump structures in some layers. (Fig. 6.) The excellent exposure of the area allowed the determination of the relative slumping direction in many cases. Only in one exceptional case, close to the northern

Fig. 4. Banded meta-tuff (Bed 3). Way up direction → (Kå 292 A1 and 292 A 2).

Fig. 5. Uranium-bearing banded meta-tuff with densely laminated individual beds. Way up direction → (Kå 31/68). Compare with Fig. 19.

Fig. 6. Slump-bedding in banded meta-tuff (Bed 3).

termination of the underlying lava flows, was the transport towards the north. In all the others it tended to the south (naturally under the condition, that within the transverse section studied, the beds are always younging westwards). In connection with the slumps, an intraformational breccia occurs occasionally.

The lighter coloured beds of banded meta-tuffs consists chiefly of quartz and plagioclase. The relative proportion of these minerals is very variable, both of them together make up about 40—80 per cent of the rock. There are two forms of quartz grains. The first one, more characteristic of the light beds, represents fairly elongated lenticles which are up to 2.5 mm in size at the bottom of the bed. The average size is approximately 0.5 mm. The less frequent second type are the sharp outlined, splinter or wedge shaped grains. Plagioclase is in general fairly altered to epidote, making an accurate determination, almost impossible. Albite occurs for the most part in small amounts. The green hornblende comprises commonly about 20—30 % of the rock. If biotite appears, it occurs close to the boundary between the light and dark beds, hornblende is subordinate. Muscovite is also an occasional component but is not as significant as sphene.

One of the peculiar features of the tuffs in question are the laminae consisting almost exclusively of fine epidote aggregates, which occur on the boundaries of light and dark beds. The thickness of these laminae is 0.2—1 mm.

The d a r k b e d s of banded meta-tuff display an average grain size of approximately 0.1 mm. Their main component is an iron-rich biotite occurring as minute flakes, greyish brown to opaque in colour. Pleochroic haloes occur in the biotite around extremely fine ore inclusions. Chlorite, hornblende and quartz are markedly subordinate to biotite. Epidote and sphene are closely associated with biotite forming together flocculent aggregates, but epidote also forms zoned and cloudy crystalloblasts, up to 0.7 mm in size. Ore minerals show a tendency to concentration in the dark beds.

In addition to the more or less regular beds, there are also frequently apparent schlieric layers, very dark green in colour, being commonly conformable to the bedding, but very often passing into ptygmatic veinlets. The veinlets are sharply restricted towards light and dark beds. They consist of coarse grained hornblende, green in colour with γ/c angle 26—28°. Other minerals, such as epidote, quartz, colourless mica, sphene and ore are accessories. It seems very likely that these aggregates are due to metamorphic mobilization.

Table 5 gives the mineral composition of the non-mineralized banded meta-tuffs and other rocks expressed in per cent volume. The bulk chemical composition of the banded meta-tuffs is given in Table 4b.

2.4. QUARTZ-BIOTITE SCHISTS (BED 4)

The quartz-biotite schists of Bed 4 are very fine-grained, diffusely stratified, with very clear lamination, and in certain places with a pronounced graded bedding or cross-bedding. The rocks are dark greyish brown on a freshly broken surface, light greyish brown, yellowish brown or rusty weathering. In the uppermost horizon of the unit, many small white cherty lenses are scattered within the quartz-biotite schist. The contact with the overlying unit is distinct and sharp while the transition to the underlying banded meta-tuffs is successive.

The mineral composition of the quartz-biotite schist is rather simple. They are composed of very fine-grained quartz, light brown biotite, muscovite, plagioclase, epidote and accessories, but the strongly dominating components are quartz and biotite. In transitions to the banded meta-tuffs, light green amphibole appears. Microscope investigations permitted the distinction of two types of schist and displayed the essential differences in their textures and mineral composition. The schist of the first type has a grano-lepidoblastic texture and consists of a fine-grained mosaic of quartz, albite and biotite which exhibits a parallel alignment. Epidote is accessory or absent. In the schist of the second type, which has a clasto-blastic texture, the quartz grains form a disrupted framework filled with biotite, muscovite and plagioclase which is almost completely replaced by epidote. A common accessory in both types of schist is tourmaline, in places being gathered into thin layers or schlieric aggregates. Sphene is less abundant, zircon — very rare. Pyrite is sparsely disseminated throughout the schists and sometimes

concentrated in thin layers or patches. It intergrows with epidote and is often enveloped by chlorite. It is notable however, that chlorite occurs exclusively in connection with pyrite.

2.5. REMARKS ON A DEVELOPMENT OF BEDS 2—4

Though the rocks of the lower part of Formation A have been metamorphosed largely to the greenschist facies, relict textures and structures permit some conclusions concerning their genesis. The top of the lava flow and the graded bedding of the tuffs indicate the western direction of "younging" in the whole unit. Taking into account the distinctly sharp boundary with the overlying Bed 5 and composition of the stratigraphic sequence (the lava flow on the bottom, overlain by tuffs with an increasing quantity of clastic components in direction of "younging") it is possible to presume that Beds 2, 3 and 4 represent a simple volcanic-sedimentary cycle. A sub-aqueous environment for deposition is indicated by the mafic character of the lava, pillow-like structures and the form of bedding of the tuffs.

Within the exposed section in the map area, the direction of deposition of the volcaniclastic rocks is from north to south. This is deduced from the increasing thickness of the rock sequence southwards and the observations of slumping.

With reference to the relatively high sulphur content of the rocks, it is possible to speculate that a brisk exhalative activity immediately followed, and to a small extent preceded volcanic explosions. In the same way, the quartz-rich rocks can be explained by the crystallization of silica gel derived from volcanic silica, contributed to the sea, and deposited concurrently with the associated pyroclastic particles.

3. FORMATION A, BED 5—BED 7d

The upper part of Formation A, which overlies with a relatively sharp contact Bed 4 and in the northern part Bed 3, is composed of four units — Beds 5, 6, 7c and 7d. Bed 5 and Bed 7d comprise tuff breccia, tuff, graphite-bearing tuffite, cherty tuff, graphite schist, chert and marl. Beds 6 and 7c consist of volcaniclastic psephitic rocks with associated schlieric or banded tuffs and to a small extent interbeds of graphitic tuffite. All the rocks have been metamorphosed largely to the greenschist facies, thus no primary mineral assemblages are fully preserved.

Beds 7c and 7d extend in the northern part of the area from Formation A into Formation B, appearing there as a tongue between contemporaneously deposited sediments. Their contacts towards surrounding sediments will be discussed later. From the petrological point of view, the rocks composing Beds 5 and 6 are identical with the rocks of Beds 7c and 7d, but they appear in an inverse stratigraphic order.

The rocks of Beds 5 and 7d are represented very unevenly. There are no sharp

boundaries between them, the meta-tuffs and tuffites form a matrix in which the lenses of chert and interbeds of the graphite schist are embedded. This situation is demonstrated in detail in Fig. 21 and Plate 4. Compared with others, the rocks of Bed 5 are more schistose and scapolitized than any other rocks of the area studied.

The uranium mineralizations only occur within Bed 5 and Bed 7d, being connected entirely with graphite-bearing rocks and chert. Sulphide minerals also occur in Bed 6 but in smaller quantities.

3.1. META-TUFFS AND ASSOCIATED ROCKS OF BEDS 5 AND 7d

The greenschists of Bed 5 and Bed 7d are greenish brown or rusty weathering rocks, dark greenish grey on a fresh surface. They often are distinctly layered or laminated. Banded rocks with alternating darker and lighter bands, similar to those of Bed 3 are rare. Frequently present are recognizable transitions to meta-psephitic rocks or graphite schist. An accurate petrographic classification of the rocks is difficult to make because of the large extent of greenschist alteration and comparatively intensive scapolitization. Nevertheless, two rock varieties are easily recognized, viz. meta-tuffs and graphite-bearing meta-tuffites.

3.1.1. Meta-tuffs

In mineral composition, the non graphite-bearing meta-tuffs are similar to the banded tuffs of Bed 3 but mostly lack the regularity of structure. Graded bedding hos not been observed, the separate laminae grade into each other and differ only in the relative abundance of green hornblende, albite and quartz. In the rock as a whole, biotite is dominant over hornblende. Epidote is either scattered haphazardly or gathered into thin laminae. Muscovite, sphene, tourmaline and ore are accessories. Close to the chert bodies, the amount of quartz and muscovite increases in the tuffs while that of biotite and albite decreases. Cherty tuffs develop as a transitional rock here.

3.1.2. Graphite-bearing meta-tuffites

Graphite-bearing meta-tuffites, provided that they are not perceptibly mineralized, differ from the above rocks partly in structure and in the presence of graphite which is either disseminated throughout the rock or gathered into thin laminae. The amount of graphite varies considerably, from traces to approximately 1 % of the rock, but averaging 0.04 %. The meta-tuffites are mostly very fine-grained, diffusely stratified or massive, rarely graded bedded. Original internal structures are mostly obliterated by strong cleavage. No pronounced banding is apparent. Under the microscope, the rocks are composed of biotite, amphibole and epidote. Quartz, graphite, sphene, carbonate, sericite and scapolite occur in

minor amounts. Biotite is coloured brown or dark brown. Quartz mostly occurs only in association with biotite, being at the same time more abundant in the parts where biotite is considerably lighter in colour. In addition to extremely fine-grained green or sooty green hornblende, actinolite amphibole appears frequently. It is often needle-shaped and gathered into thin laminae where the grains may, in certain places, form fan-like aggregates.

Transitional rocks between the graphite-bearing meta-tuffites and the graphite schists are well stratified with alternating laminae consisting of quartz, biotite and varying amounts of graphite. In places there occur small lenticles made up of quartz, large albite porphyroblasts and some biotite.

3.1.3. Graphite schist

Graphite schist is best characterized as an extreme variety of graphitic meta-tuffites. The rock is greyish black, well bedded or laminated, but frequently strongly folded in detail and brecciated. Thin layers with graphite contents up to 7.6 % of the rock alternate with laminae which consist of coarser grained aggregates comprising quartz, quartz-albite or quartz-albite-biotite. Colourless or yellowish white chlorite often appears besides the biotite.

3.1.4. Fragment-bearing rocks

The irregular layers of fragment-bearing meta-tuffs occur frequently inside the rocks described above. The fragments are sparsely disseminated in the rock and in the present stage of the recrystallization, there is no difference in the mineral composition of the fragments and the surrounding rock. A particular feature of these rocks are minute layers, which consists of albitophyre fragments embedded in an albite-biotite matrix. The size of fragments is 0.5 to approximately 5 mm. They are mostly stretched and flattened out in the schistosity plane so that their original form is not preserved. The albitophyre is a very fine-grained rock of allotriomorphic texture with accessory muscovite, epidote and actinolite amphibole.

Meta-t u f f - b r e c c i a which forms a thin horizon with a sharp contact towards the underlying quartz-biotite schist, occurs in a few places at the very bottom of Bed 5. The length of these breccia bodies is about 200—400 m, the thickness does not exceed a few metres. The agglomeratic structure is apparent only on the weathered surface. On a freshly broken surface the rock is blackish green. Both the fine-grained groundmass and closely packed angular fragments have the same mineral composition. They consist of a fine-grained hornblende-epidote aggregate. The hornblende is light green or bluish green in colour (γ/c — 27°), exhibiting often an euhedral form of crystals. Muscovite and titanite are accessories.

3.1.5. Meta-chert

Meta-chert occurs in the form of flasers or irregular layers, which are from a few decimetres to approximately 1 100 m long and up to 30 m thick. It is a grey, or rarely pink, chalky white weathering rock which is laminated and banded in places (Fig. 7), but for the most part is structureless. A brecciated structure is rather unusual. Zones of sooty black (rusty weathering) sulphide-bearing chert are mostly developed along the margins of the larger lenses or layers.

Under the microscope a mosaic texture of the massive chert is apparent and its two textural types are discernible. The first one, where the mosaic is composed of irregular, lobate or jagged grains (Fig. 9A), and the second type — foam texture with sharp and roughly straight restricted quartz grains — resulting from recrystallization of the first type (Fig. 9B). In addition to quartz, the rock consists of hornblende (frequently in subhedral form), clinozoisite, biotite, muscovite and sphene. The banded chert is composed of alternating coarse- and fine-grained layers, which range in thickness from hardly perceptible laminae up to a few centimetres thick (Fig. 9C). The form of quartz grains is comparable with that of the massive chert. Biotite, muscovite, epidote and actinolite amphibole appear more extensively, forming up to 20 % of the rock. They are mostly gathered in laminae which grade into the quartz beds. If ore minerals occur, they are associated with biotite and amphibole. Especially on the contacts with surrounding rocks, the chert beds alternate with thin tuff laminae (Fig. 8).

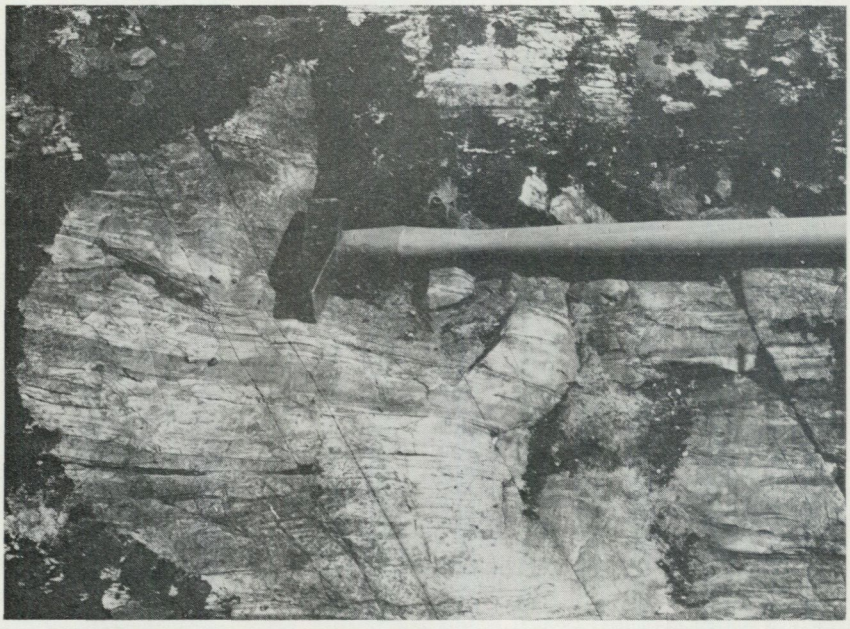

Fig. 7. Banded meta-chert. The banding is only due to the alternation of coarser and finer grained layers (Bed 5).

Fig. 8. Banded meta-chert. The banding is due to intercalations of a basic meta-tuff (Bed 7d).

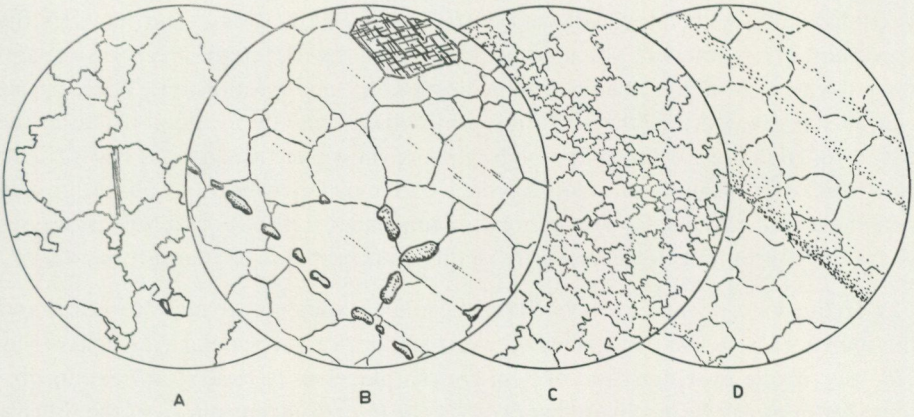

Fig. 9A: Massive chert of a mosaic texture with lobate and jagged quartz grains. Acessories are muscovite and sphene. 1 nic., 45 x (Kå 40/68).

B: Massive — recrystallized — chert of a foam texture containing subhedral hornblende crystals and grains of sphene, the latter being partly arranged into a string-like aggregate. 1 nic., 45 x (Kå 39/68).

C: Banded chert with alternating coarser and finer laminae. 1 nic., 18 x (Kå 308/69).

D: Magnetite-bearing banded chert. Magnetite is gathered into very thin laminae whose microstructure suggests graded bedding. 1 nic., 65 x (Kå 58/68).

3.1.6. Meta-marl

The meta-marl was detected by only one drill hole, Kå-70003, where it formed a layer at least 2.5 m thick (Fig. 21). The rock is light grey, distinctly bedded with alternating layers consisting of an impure carbonate and of a silicate mixture. The thickness of the individual layers is very varyable.

Under the microscope, largely flattened grains of a carbonate appear as the main component. Colourless or yellowish chlorite of a sheridanite type, tremolitic amphibole and light brown biotite occur in minor amounts. Zircon, clouded plagioclase and opaques are accessory. The whole rock analysis assayed, after leaching with 1N—HCl at room temperature, 10.3 % Ca, 1.6 % Mg, 2.4 % Fe and 0.2 % Mn in the soluble part, and 52.2 % of an insoluble remnant. The CO_2 content was 13.8 %. The carbonate present seems to be dolomitic calcite.

3.2. META-VOLCANICLASTIC PSEPHITE (BED 6 AND BED 7c)

A complex of coarse fragment-bearing rocks associated with meta-tuffs and graphitic meta-tuffites is one of the most conspicuous parts of the unit described. It appears in the whole central part of the greenschist belt, where it is fully conformable with the underlying rocks, but its upper, i. e., western contact is mostly tectonically modified and therefore it seems slightly discordant with the overlying stratum. But it is still evident that the transition to younger sediments was gradual and without any interruption.

The name meta-volcaniclastic psephite is proposed for the fragment-bearing rocks which display an average fragment size more than 2 mm. The name used is conformable with the classification of Fischer (1961, 1966), and includes the spectrum of fragmental volcanic rocks formed by different mechanisms and mixed with any non-volcanic fragment types in any proportion. These rocks can be sub-divided into three groups, which differ mainly in their structure, the nature of matrix, and the shape of fragments (however, it is sometimes difficult to deduce the original form of fragments as they have been in places greatly deformed and flattened). The groups distinguished refer to different processes of fragmentation but not necessarily to different processes of deposition.

a. In the meta-p y r o c l a s t i c b r e c c i a the fragments are closely packed and the matrix merely fills the spaces between angular or subangular fragments (Fig. 10). No sorting is evident and only in certain places is a crude stratification present. As far as can be discovered at present, the interstitial substance of the breccia was originally a tuff. Preserved phenocrysts of an albitized plagioclase indicate the occurrence of a crystallic tuff. Besides plagioclase this meta-tuff contains actinolite amphibole and epidote. Quartz and very fine rock fragments are less common.

The pyroclastic breccia enriched in carbonate represents a special variety of the rocks under consideration. On the surface, the fragmental nature of this rock

Fig. 10. Pyroclastic breccia (Bed 6).

is mostly masked by a pocky weathering. More or less carbonatized fragments are embedded in a matrix that consists of hornblende, epidote and biotite. Calcitic carbonate makes up the rims around the fragments or minute lenticles.

b. The meta-l a p i l l i t u f f (Fig. 11) is in general finer grained than the rocks of the former group. It is an open-framework rock, greyish green in colour. Lensoidal, elliptical, subangular or spindel-like lapilli are often zoned, mostly with lighter rims. The lapilli are embedded in a matrix consisting of abundant submicroscopic fragments. In most outcrops, little or no sorting is evident, although a stratification is nearly always present. The mineral assemblage of the matrix is similar to that of the first group. In certain places isolated large ovoid lava bombs occur together with lapilli. The bombs are of spheroidal structure and range from 1 dm to as much as 60 cm in diameter.

c. The meta-s h a r p s t o n e c o n g l o m e r a t e o r t u f f - c o n g l o m e r a t e (Figs. 12 and 13) of the third group is an open-framework polymict psephite whose matrix may be described as meta-tuffite. The rock is composed of angular to rounded fragments averaging 2—5 cm in size. The fragments generally do not display a zoning structure. Stratification is always present and in some outcrops an advanced state of sorting is apparent. The sharpstone conglomerate is a characteristic rock of Bed 7c.

The petrological character of the fragments is the same in all these rocks. Porphyrite is most frequent in the pyroclastic breccia and lapilli-tuff. Chert and

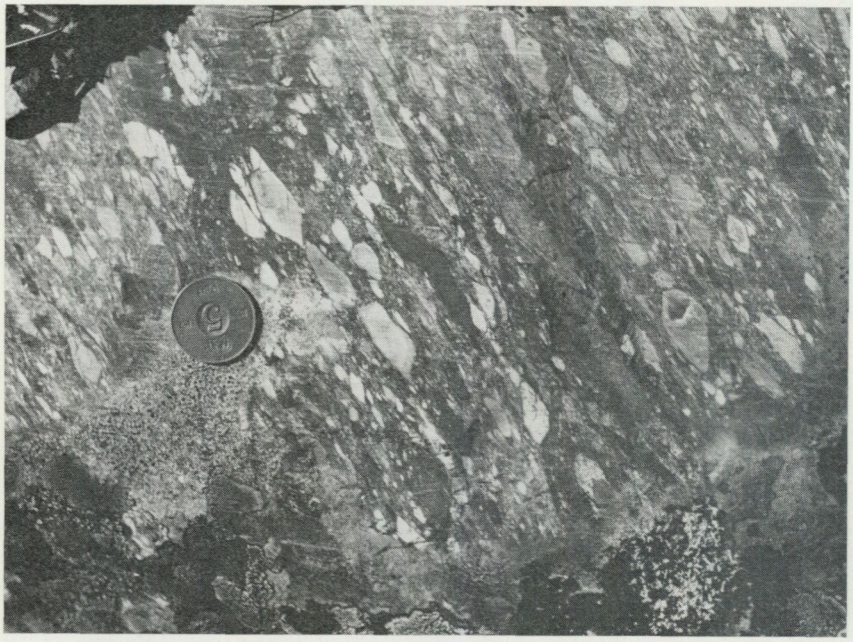

Fig. 11. Lapilli tuff (Bed 6). The coin is 2.7 cm in diam.

fine-grained tuffs are less common. In the sharpstone conglomerate, chert prevails over porphyrite but the relative abundance of different rock types varies considerably from place to place. The fragments forming porphyrites are very fine-grained with an almost affanitic groundmass which consists of albite, hornblende and epidote. Quartz, calcite and opaques are accessory. The amount of hornblende varies from very little to more than 50 % of the rock. In places a statistical pattern of the albite columns is apparent. Phenocrysts which consist of albite bands manifest in some fragments a fluidal arrangement. Larger irregular and riddled albite grains with more basic "blebs" are rather common. The degree of porphyrite alteration varies considerably. Euhedral zoisite porphyroblasts are exclusive components of some fragments. Chilled rims are frequent in porphyrite fragments, regardless of their size.

Special notice is paid to chert lenses within a meta-psephite. The size of chert bodies ranges from a few centimetres to more than 1 m. They are mostly strongly deformed and terminate abruptly, in other cases they pinch out gradually along the strike. These chert bodies might be interpreted as a disrupted bed. In one case, the red jasper has been found in the uppermost part of the psephite unit, forming a few centimetres thick intercalations within the sharpstone conglomerate.

The open-framework of the majority of the rocks described suggests simultaneous deposition of fine and coarse fraction, although their stratification,

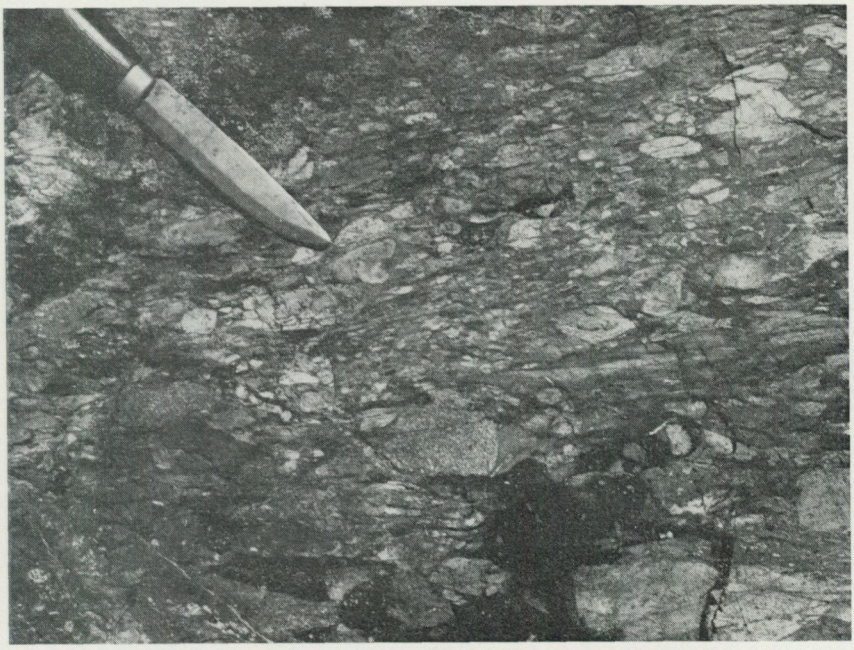

Fig. 12. Sharpstone — conglomerate (Bed 7d).

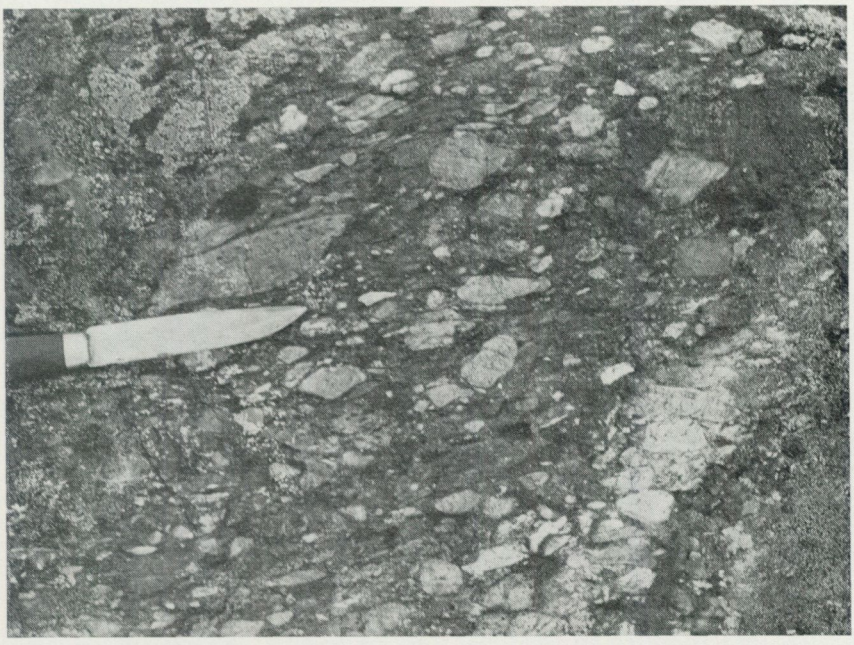

Fig. 13. Sharpstone — conglomerate (Bed 6).

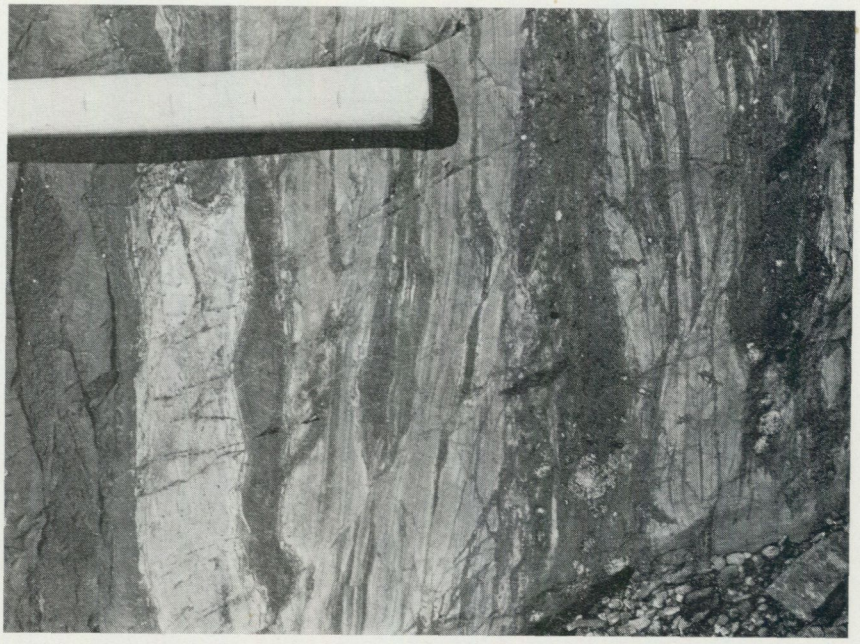

Fig. 14. Layered meta-tuff occurring in association with meta-volcaniclastic psephite (Bed 6).

occasional sorting and chert or jasper intercalations are sufficient proofs of a sedimentary aquatic origin.

Layered meta-tuffs associated with meta-volcaniclastic psephite are more abundant in the upper part of the unit and especially in its southern part. The mineral composition of these tuffs strongly resembles the non-mineralized rocks of Bed 3, however their structure is quite different. They are distinguished by irregular, schlieric bands, blackish green in colour, very often showing a zonal structure (Fig. 14). The border of the schliers is darker whilst the central part is lighter, coarser grained and enriched in epidote and albite. Graded bedding is absent. Common slump structures indicate a southerly transport of the pyroclastics within the depositional area, i. e. in the same direction as has been established for the tuffs of Bed 3.

Intercalations and lenses of graphite-bearing meta-tuffites are a more exclusive part of this horizon. In petrology, they are completely similar to the graphite-bearing tuffites already described.

4. FORMATION B

The quartzite and sandstones, which are developed in thicknesses of 30—210 m at the base of Formation B, extend along the whole Kopparåsen Greenstone Belt. As has already been described, the volcaniclastic rocks of Beds 7c and 7d

(Formation A) form a tongue within these sandstone in the northern part of the area. Consequently, the lowermost quartzite horizon of Formation B is to be found in direct contact with volcaniclastic rocks of Bed 6. This contact is distinguished by a conglomerate which is fairly deformed and some of its structural features are obliterated. Nevertheless, it is obvious that the sediments of Formation B succeed the underlying greenstones without any interruption in deposition (Fig. 15). The conglomerate itself is an open-framework rock with subrounded, but mostly stretched and flattened pebbles of chert and jasper. Greenstone and porphyry pebbles are rare. The matrix is quartzitic, in places showing a pronounced stratification. The conglomerate is overlain by a light

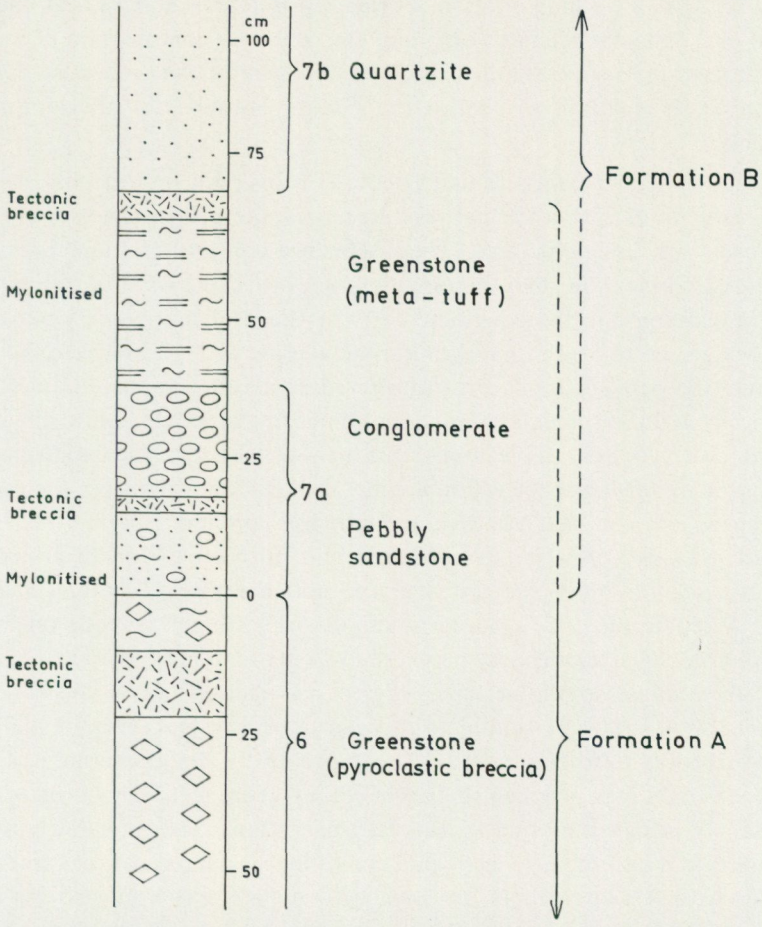

Fig. 15. Measured section through the contact of Formations A and B, exposed west of the hill Kuokkel. The section demonstrates a gradual development of Formation B from Formation A, without any interruption in deposition. The present tectonic disturbances reflect merely the behaviour of differently competent layers during folding. They do not represent any large scale dislocation.

quartzite which passes into quartzitic sandstone. Both the rocks are well stratified. In addition to quartz, they consist of muscovite, altered plagioclase, actinolitic amphibole, epidote and tourmaline. The amount of unstable and new formed minerals is very variable but does not exceed 25 % of the rock. These minerals might be interpreted as a pyroclastic admixture, at least to a certain degree.

Both the top boundary of Bed 7d and the bottom boundary of Bed 7c grade into the surrounding sandstones. In the lower part, there are thin sandstone layers alternating with beds of the sharpstone conglomerate. By the upper contact, a thin conglomerate horizon appears in places within the sandstones neighbouring the meta-tuffs of Bed 7d. There is no indication that a discordance exists between Formation A and the lowermost part of Formation B. In conclusion, then, one can say that the lowermost units of Formation B represent a radical change in the type of sedimentation, but with a contemporaneous continuation of the pyroclastic process of fragmentation. Excellent exposure of the area does not allow any tectonic speculation to change the picture outlined for the stratigraphic succession.

The sandstone and quartzite unit (Bed 7b) is overlain by a pebbly sandstone bed reaching up to 250 m in thickness. In places, the pebbly sandstones become open-framework conglomerates. The fragments comprising these rocks show considerable elongation, they are spindel-like, but if the original shape is preserved (mostly only in the conglomerate) they have high sphericity and roundness. They are up to 35 cm in length but the average is 3—25 mm. In the pebbly sandstone, the pebbles are formed of altered porphyrite, quite similar to rocks which occur in the volcaniclastic meta-psephite. In the conglomerate, the cobbles of quartz-porphyry are a substantial constituent of the rock. The quartz-porphyry itself is grey, reddish grey or red in colour. Under the microscope, the porphyry is composed of a microcrystalline groundmass containing numerous, usually well individualized phenocrysts of quartz and microcline. In the groundmass, there also occur albite, oxidized hematite and accessory biotite, sphene and apatite. A replacement by epidote is less intensive than has been observed in the porphyrite. Quartz-porphyry pebbles has been found in Beds 7a and 8, but not in any other lithostratigraphic unit, older or younger. However the rock under consideration is strikingly similar to the quartz-bearing porphyry of the Kiruna area described by Offerberg (1967). The matrix of the conglomerate and pebbly sandstone is light grey or greenish grey in colour. It seems to have been originally composed of subangular quartz and feldspar grains, but it is fairly well recrystallized to a granoblastic aggregate consisting of quartz, epidote and colourless mica with feldspar relicts. In some beds quartz makes up less than 50 % of the rock. Thus the original rock is more accurately called a pebbly subarkose, however a less specific but perhaps more descriptive field name is preferred.

Well-stratified or laminated greenstones (Bed 9) overlie the pebbly sandstone. An interesting feature is the presence, in only one bed, of cross-bedding which

indicates the westward direction of younging. Both internal structured and psammitic texture are evidence of a hyaloclastic nature for the initial rock type.

The sedimentary and volcaniclastic rocks of Beds 7a, 7b, 8 and 9 probably form a sedimentary-volcanic cycle which is abruptly terminated.

The greenstones of Bed 9 are overlain by sandstones which pass upwards into a pebbly sandstone and a greenstone (Beds 10—12). A number of sedimentary structures indicative of shallow, turbulent waters are apparent within the sandstone. Minute erosion channels on certain bedding planes are note-worthy. In all cases the structures indicate younging of the beds towards the west. The stratigraphic succession of Beds 10—12 is in complete agreement with the previous cycle and can be regarded as a new cycle.

The uppermost unit of Formation B, comprising sandstone and pebbly sandstone, is exposed in a narrow belt coinciding with a shear zone parallel to the strike of the rocks. The highly schistose and minutely folded rocks along the western boundary of the unit, grade into essentially unsheared rocks on the eastern side of the belt. The western contact itself is made up of a dislocation that functioned during the ultimate stage of development as a normal fault. The hanging wall of this fault is partly made up of caledonian rocks of the Torneträsk Group.

5. META-PORPHYRITE SILLS

A well defined group of sills is situated within the rocks of the upper part of Formation A. One small sill also occurs on the contact of Bed 11 and Bed 12 in Formation B. The largest sill occurring in Formation A is 2 950 m long and up to 125 m thick. It is underlain and overlain by meta-psephite and as a rule, has fine-grained margins at the contact with the wall-rocks. Several thin layers of meta-tuff lie within this sill and strike almost parallel with it walls. Apparently they have not been deformed by emplacement of the sill. But in other places near to the sill contact it has been observed that the surrounding rocks are slightly disturbed and the sill itself brecciated.

On weathered surfaces the rock is coarse-grained, porphyritic, with large blocky hornblende phenocrysts that give the rock a mottled appearance (Fig. 16). The typical sill rock seems to be composed of about 40—50 % hornblende and 50—60 % greenish altered feldspar. On the surface of the drill core a spotted structure with dark brownish green, 0.1—0.5 cm in size, diffusely defined spots of hornblende and biotite is apparent in a light grey groundmass.

On a freshly broken surface, the rock is massive and it is difficult to recognize any individual crystals. In places, the variations in grain size and the preferred orientation of dark spots produce a distinct banding.

In well preserved parts of samples from a drill-core, porphyritic texture is apparent under the microscope. The texture is mostly affected by later recrystallization which cause the rock to become schistose with bands rich either

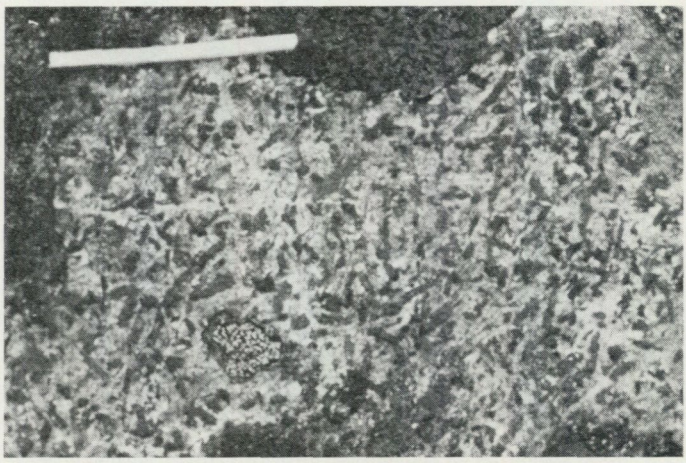

Fig. 16. Meta-porphyrite sill showing blocky amphibole megacrysts in the groundmass of altered feldspar. (The match is 5 cm long.)

in biotite or epidote. The plagioclase prisms are never quite fresh but altered to a fine-grained mass of epidote, amphibole, white mica and albite. Albite occasionally appears as patches of relatively clear grains. Scapolitization is rare. The original composition of the plagioclase is mostly impossible to determine. In preserved grains it corresponds to labradorite (An_{56}). The amphibole occurs as large irregular hornblende crystal scattered in the plagioclase mass and gathered in the "spots", or as fine uralitic needles. All the varieties are very light in colour — pale green to yellowish green (γ/c angle is about 22°, but the angle of the uralitic needles is smaller). In places, many sphene inclusions appear in the (110) planes of the hornblende. (They make up as much as 10 % of the plane in the amphibole section.) The biotite is very light beige to light brown in colour. It occurs as very fine flakes scattered throughout the whole rock and as larger individuals gathered in small bands where it exhibits parallel orientation, or in the above mentioned "spots"-aggregates where it appears together with hornblende. The quartz appears as fine dispersed grains forming as much as 2—3 % of the rock, and as later mobilisates forming, together with calcite and scapolite, small veins. Interstities between the plagioclase and amphibole are occupied by the epidote, white mica and biotite mass. The only opaque mineral is magnetite which is rather abundant in places and occurs bordered with very fine-grained sphene aggregates.

6. FORMATION C

Bed 14, which is the last lithostratigraphic unit appearing in the Kuokkel Group, forms a separate unit — Formation C. It has been mentioned above that the eastern boundary of this unit is tectonic, to the west — granite sharply cuts it. Restricted in this way, the unit is exposed as a belt 180—600 m in width.

Fig. 17. Laminated greenstones, meta-volcanic turbidite. (Bed 14.)

Greenstone, is the sole component of Formation C and is somewhat similar to the rocks of Beds 9 and 12, but it is very unlike any rock from Formation A. On the weathered surface, the rock is greenish brown or rusty brown in colour showing continuous, even lamination throughout the horizon (Fig. 17). It commonly displays graded bedding, a feature accentuated under the microscope. The grading is of a type that could be described as follows: Each successive increment is similar to the proceeding, except that it contains one less coarse grade. The fines are distributed throughout. The rock under consideration is thus a disrupted framework one, in which green hornblende grains, averaging 0.3—0.5 mm in size, make up 45 % of the volume. The grains are elongated, angular or subangular and dot not show any trace of deformation. They are in places accompanied by brown biotite. It seems that the original form of the psammitic grains is thoroughly preserved. The matrix consists of a very fine-grained aggregate of epidote, colourless mica and altered plagioclase. Accessories are quartz and opaques (magnetite with sphene rims). The texture of the rock might be defined as blasto-psammitic.

A volcaniclastic character for the rock under consideration appears indisputable. It has been water-lain and represents a turbidity-current deposit. However, a more accurate definition is difficult because an epiclastic character for the fragmentation is a possibility.

III. ORE MINERALIZATIONS

1. URANIUM MINERALIZATIONS

1.1. GENERAL FEATURES OF URANIUM MINERALIZATIONS

Uranium mineralizations in the Kopparåsen area occur in the eastern and central part of the greenstone belt (Fig. 2 and Plate 2). Stratigraphically, uranium occurs at different levels of Formation A but always confined to this formation. From the point of view of geometry, three types of occurrences may be distinguished:

a. Disseminated uraninite forming irregular strata-bound mineral concentrations* connected with Beds 3, 5 and 7d.
b. Uraninite associated with skarn-like metamorphic mobilisates at different stratigraphic levels.
c. Veinlets of uraninite associated with minor faults or joint sets.

As the bedrock throughout the investigated area is well exposed and the uranium has been shown to be in good equilibrium with its daughter-products, the distribution of the uranium mineralizations can be easily studied by the help of radiometric measurements on the ground. The following description of the distribution of the uranium mineralizations is thus mainly based on such measurements. The main uranium mineralizations appear in two belts, viz. Beds 3 and 5 while minor mineralizations occur in Bed 7d. In the map showing radioactive anomalies (Plate 2), all anomalies displaying a radioactivity of more than 100 μR/h are included. Some of these anomalies are of greater size while the majority of them have small dimensions or are only spots. Random samples taken from places of highest radioactivity and drill-core samples have assayed 0.01—1.28 % of uranium and only traces of thorium (Adamek 1973).

The delimitation of the mineral concentrations is somewhat arbitrary as the uranium mineralization passes gradually into the host rock. The mineralized bodies have an alongate, lenticular or elipsoidal form, sometimes very irregular in detail, whose longest axes are in exposed sections almost always conformable with the bedding of the rock. The mineralized bodies are in fact composed of sets of continuous uraninite-bearing seams, each of them being between 1 and 10 mm thick. These seams are regular and perfectly conformable to the bedding of the surrounding rocks. Even when the rock is slump-bedded, which is frequently the case in Bed 3, the mineralized layers follow the disturbed beds (Fig. 18).

* The term "mineral concentrations" is used in this account as meaning a mineralization at least 10 m long with a uranium content of more than 0.01 %.

Fig. 18. Photo (left) and autoradiogram (right) of the uraninite-bearing banded meta-tuff of Bed 3. Observe the minute slump-fold in the upper left of the specimen. Pyrite is white on the photo and uraninite white on the autoradiogram. Natural size. Way up direction ⟶ (Kå 31/68, anal. no. 001—2020; 0.094 % U. Compare with Fig. 4.)

1.2. SOME COMMENTS ON THE COMPOSITION OF THE HOST ROCKS

The banded meta-tuffs of Bed 3 endowed with a richer uranium mineralization exhibit slight differences in mineral composition as has been revealed through microscope investigations. In contrast to the unmineralized meta-tuffs where chlorite mostly occurs only in minor amounts, green chlorite is frequent close to uranium mineralizations. The chlorite occurs as scattered fine flakes or is gathered in small schlieren-like aggregates in which it appears in association with quartz, biotite, sulphides, sphene and occasionally also fluorite. Besides chlorite, carbonates occasionally occur in the form of disseminated grains, patches or small diffuse veins. In certain layers, the break-down of iron-rich biotite into a new mica, light in colour and slightly pleochroic, has been observed as well. This mica has probably a phlogopitic composition. A somewhat puzzling feature of the mineral assemblage described is the occurrence of plagioclase grains of andesine composition which, in contrast to most of the plagioclase of the rock, are essentially unaltered.

The variation in mineral composition of uranium-bearing banded meta-tuffs is demonstrated by recalculations of chemical analyses according to Köhler, Raaz (Fig. 20). Chemical analyses were made of composite samples composed of two to nine random samples whose concurrent mineralogical composition was previously revealed through microscope investigations. The results of the

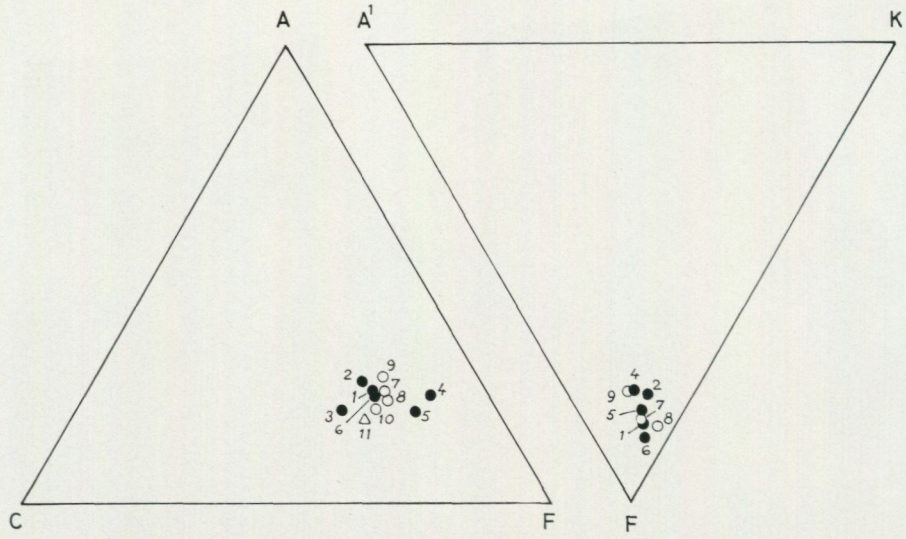

Fig. 19. A-C-F and A′-K-F diagrams (atomic proportions) of rocks from the Kopparåsen greenstone belt. Chemical analyses used for plotting are shown in Tables 4 a—c. 1—6: uranium-bearing banded meta-tuff from Bed 3; 7—10: barren banded meta-tuff from Bed 3; 11: uranium-bearing graphitic meta-tuffite.

$A = Al_2O_3 + Fe_2O_3 - (Na_2O + K_2O)$ $A' = Al_2O_3 + Fe_2O_3 - (CaO + Na_2O + K_2O)$

$C = CaO$ $K = K_2O$

$F = MgO + FeO + MnO$ $F = MgO + FeO + MnO$

No corrections have been made.

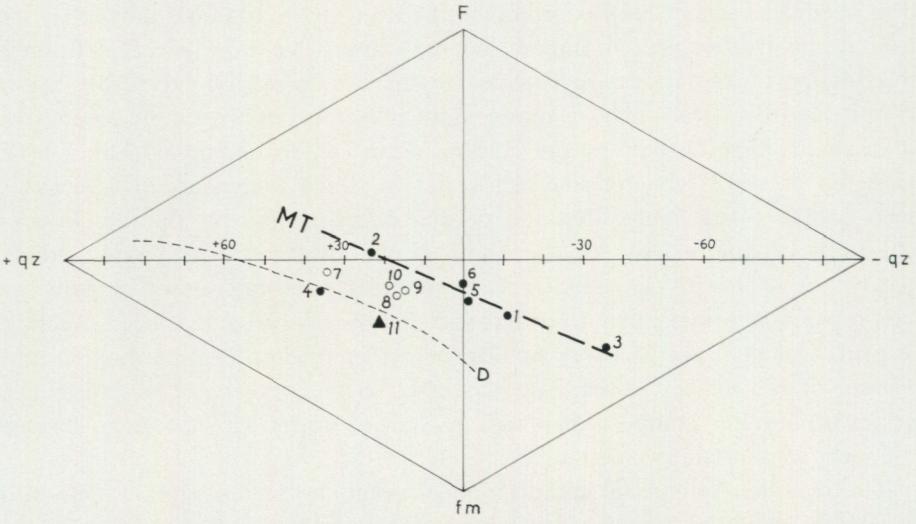

Fig. 20. Chemical composition of uranium-bearing banded meta-tuff (1—6), barren banded meta-tuff (7—10) and uranium-bearing graphitic meta-tuffite (11) shown in a diagram after Köhler, Raaz (1951). Dashed line MT — trend of the uranium-bearing meta-tuff; dashed line D — approximate boundary between sedimentary and igneous rocks after Bouska (1968). Rock analyses are set up in Tables 4 a—c.

analyses in "raw" and "transformed" values are shown in Table 4a, Figs. 19 and 20. There is a quite close congruence between the calculated average chemistry of the uranium-bearing and barren banded meta-tuffs. With the exception of analysis No. 4, representing fine-laminated meta-tuff resembling the quartz-biotite schist of Bed 4 (relative enrichment in Al together with high +qz show marked sedimentary character of this rock), the analyses of uranium-bearing meta-tuffs display enrichment in the femic component (fm-value of Köhler-Raaz showing femic cations and Ca bound in micas, amphiboles etc.). Uranium exhibits a trend towards concentration in the rocks undersaturated in quartz (—qz). The analyses Nos. 1, 2, 3, 5 and 6, showing high variation of the total chemistry, are in Köhler-Raaz's diagram arranged along one trend line. It might be assumed that these analyses reflect the originally varied and more basic petrochemical character of the uranium-bearing meta-tuffs, and, this variation is probably not caused by a later alteration.

In Beds 5 and 7d, the uranium mineralizations are mostly associated with graphite-bearing rocks (Fig. 21). On the other hand not every graphite-bearing rock is uranium-bearing and no obvious correlation between graphite and ura-

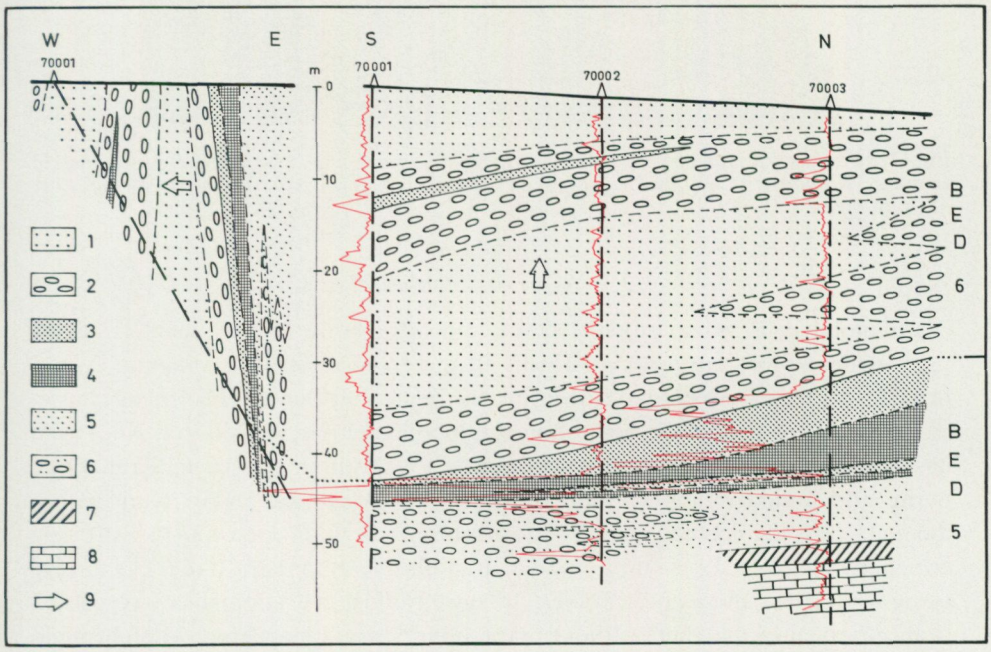

Fig. 21. Sections through the contact of Beds 5 and 6 in the northern part of the area. The longitudinal section (right) has a 60° inclination to the horizontal plane. Profiles of the radiometric well-logging show the distribution of uranium mineralizations.
Legend: 1 — layered, in places laminated, meta-tuff; 2 — meta-psephite (pyroclastic breccia, lapilli-tuff, sharpstone conglomerate); 3 — graphitic meta-tuffite; 4 — graphite schist with meta-chert intercalations; 5 — meta-tuff; 6 — fragment-bearing meta-tuff; 7 — meta-chert; 8 — meta-marl; 9 — way up direction.

nium has been observed. All the mineralized rocks of Bed 5 are to varying degrees scapolitized. The scapolite appears as light coloured rounded porphyroblastic aggregates up to a few millimetres in size, mostly arranged along foliation planes. The rock affected has a spotted appearance. In thin section scapolite's outlines are quite irregular, ragged, and the grains contain a large number of inclusion of mica, quartz and feldspar (Fig. 27, above). The scapolization processes are assumed to have been caused by a deep seated magmatic source, Lina granite according to Geijer (1931). It should be noted, that except for scapolite, no other minerals which clearly demonstrate effects of a granitization have been observed. Occasionally, amphibole crystals are replaced by biotite, but considering that the amphibole can represent relicts of primary minerals its transformation to biotite may be interpreted in more than one way.

In the fragment-bearing meta-tuffs, there rarely occur fragments which are markedly enriched in uranium, if compared with the "matrix" rock (Fig. 22).

Fig. 22. Autoradiogram of drill-core showing a fragment which is markedly enriched in uranium, if compared with the surrounding meta-tuff. Natural size. (D. h. 69007, 45.47—45.56 m, Bed 5.)

1.2.1. Skarn-like mobilisates

Mafic mobilisates, resembling the skarn, appearing in the form of veinlets, layers or irregular bodies are associated with all the greenschists of Formation A and in addition, they frequently occur inside the meta-chert lenses. The rocks consist of colourless or pale green actinolitic amphibole, epidote and quartz. Andradite has been found only in one case. Magnetite is a common opaque mineral, while pyrite and uraninite appear more seldom. The skarn-like bodies lying within the meta-tuffs are accompanied by a few centimetres thick zone which is strongly enriched in epidote. In the area studied, uraninite-bearing skarn-like rocks mostly occur within the meta-chert bodies. In fact, radioactive anomalies have never been observed in the chert without mafic minerals and magnetite. The chemical analyses of uranium-bearing chert show a strong enrichment in calcium if compared with the barren chert. As no carbonates have been observed in the unmineralized chert, calcium was probably introduced at the formation of the skarn as was also the case with the uranium. Veinlets of fluorite with some galena accompany rarely the skarn-like mobilisates.

1.3. URANIUM MINERALOGY

U r a n i n i t e is the only primary radioactive mineral identified. It occurs as rounded or irregular anhedral grains or as imperfect cubes, whose reflectance varies considerably even in the same sample (Fig. 23). Grain size is in the approximate range 0.001 to 0.1 mm. Uraninite grains are scattered more or less haphazardly throughout the mineralized seams or gathered into string-like laminae which are almost conformable with the bedding of the surrounding meta-tuff, but occasionally also cutting the individual beds (Fig. 24). In the

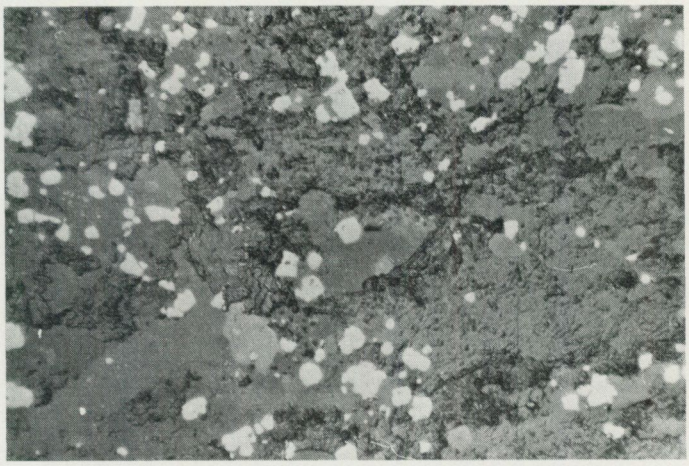

Fig. 23. Uraninite, in the form of imperfect cubes and anhedral grains, disseminated in the graphite-bearing meta-tuffite (Bed 5). Polished thin section. Reflected light, 600 x. (Drill-core 69007; 45.33 m.)

Fig. 24. String-like aggregates of uraninite in the graphite-bearing meta-tuffite (Bed 5). Polished thin section. Reflected light, 600 x. (Drill core 69007; 45.35 m.)

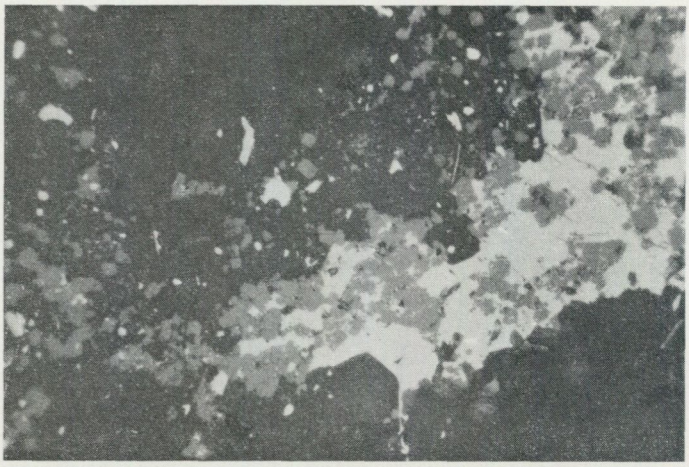

Fig. 25. Uraninite, pyrrhotite and silicate intergrowths in the graphite-bearing meta-tuffite (Bed 7d). The uraninite (grey) penetrates grain-boundaries of the pyrrhotite and appears within the pyrrhotite in anhedral or rarely subhedral form. Enveloped by silicates, the uraninite appears also in the euhedral form. The pyrrhotite surrounds and delineates uraninite grains. Pyrrhotite outlines are wholly subordinated to crystal faces of silicates. A texture indicating co-recrystallization of the involved minerals. Reflected light, 600 x (Kå 65/68).

banded meta-tuff of Bed 3, the laminar aggregates frequently appear on the boundaries between the light and dark beds. Uraninite gathered in these string-like aggregates shows mostly a lower degree of idiomorphism than uraninite grains scattered in the host rocks.

Uraninite rarely contains inclusions of silicates and exceptionally of a sulphide mineral (galena?). Apart from these inclusions, uraninite in Bed 3 has never been observed in direct contact with other opaque minerals while uraninite occurring in Beds 5 and 7d appears in direct contact with pyrite, pyrrhotite, galena and arsenopyrite. The following textural relationships between uraninite and sulphides can be seen under the microscope: Uraninite penetrates grains boundaries of pyrite and especially of pyrrhotite. On the contrary, uraninite grains are frequently included in pyrrhotite and appear there with anhedral or rarely subhedral form. The pyrrhotite forms an interstitial film between uraninite grains or completely surrounds the uraninite (Fig. 25). Pyrrhotite outlines are wholly subordinated to crystal faces of silicates.

Galena is often associated with uraninite. It occurs as anhedral grains adjoining uraninite grains. Galena only occurs in contact with uraninite when there are no other sulphides in direct contact with it.

Where in contact with arsenopyrite, uraninite never affects the crystal faces of euhedral arsenopyrite, but sometimes occurs as rounded inclusions.

Contrasting patterns of uraninite, sulphide and silicate intergrowths indicate a co-recrystallization of the involved minerals, i. e. the observed textures are

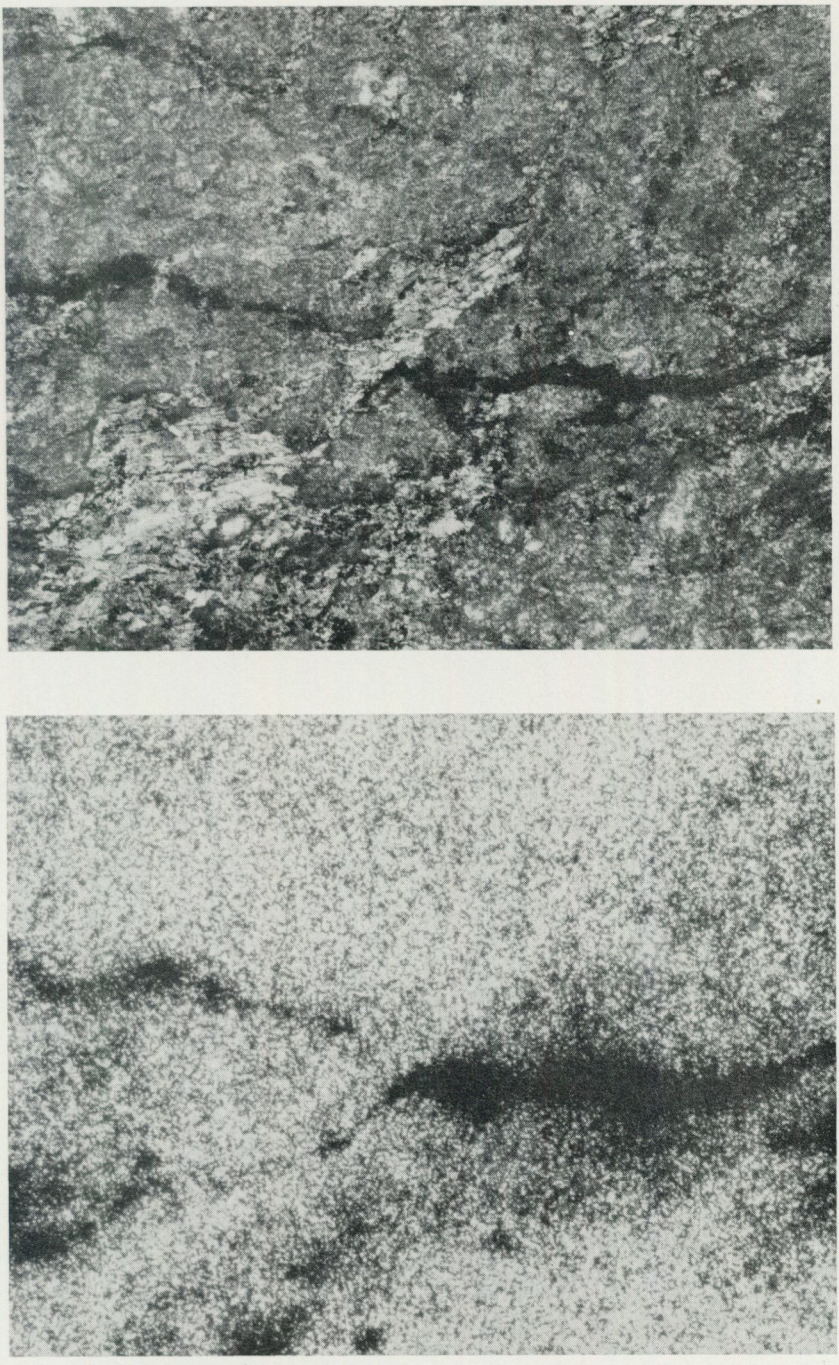

Fig. 26. Schlieren-like metamorphic mobilisates of hornblende cross-cut the laminar aggregates of uraninite. Microphoto (above) and autoradiogram (below) of the polished thin section. 1 nic., 43 x (Kå 68/68). H. Nairis photo.

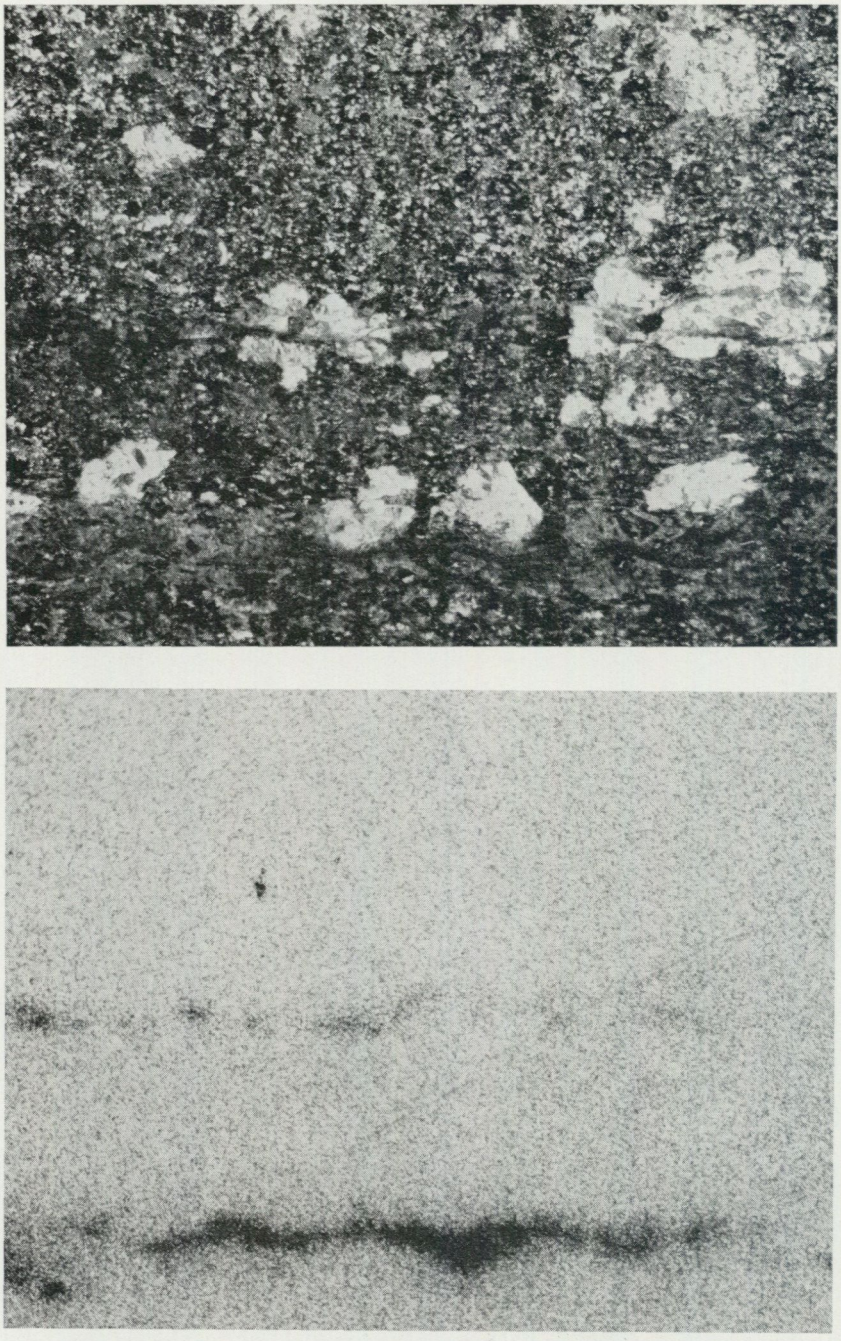

Fig. 27. Laminar aggregates of uraninite with alteration products penetrating the crystalloblasts of scapolite. Microphoto (above) and autoradiogram (below) of the polished thin section. 1 nic., 20 x. The identical uraninite aggregate with a string-like internal texture is shown in Fig. 24 as viewed in reflected light. (Drill core 69007: 45.35 m.) H. Nairis photo.

expressions of a metamorphism. The textures of magnetite and sulphides, which are even more significant, will be described and discussed in the following chapter. In recent years, these types of textures have been explained by Stanton (1960, 1964), Lawrence (1973) and others who demonstrated that they result from simple grain growth from submicroscopic aggregates, leading to coarsening, segregation of different minerals into discrete grains, and acquisition of habit in accordance with prevailing surface energy requirements.

However, uraninite also demonstrates complicated textural relationships with metamorphic mobilisates and minerals of metasomatic origin. In Bed 3, the schlieren-like metamorphic mobilisates of green hornblende cross-cut the laminar aggregates of uraninite. Uraninite never occurs within these hornblende schliers (Fig. 26). In Bed 5, laminar aggregates of uraninite, which are analogous in their form to the aggregates in Bed 3, penetrate crystalloblasts of scapolite (Fig. 27). Seen in reflected light these laminae show a string-like internal texture (Fig. 24). In the narrow zone adjoining the uraninite aggregate, the scapolite is altered into an extremely fine mass which mainly consists of white mica with some chlorite and calcite (Fig. 27).

In the skarn-like rocks, uraninite appears as fine anhedral grains mostly being gathered into thin veinlets together with magnetite. The grains contain plenty of extremely fine sulphide inclusions and larger inclusions of non-opaque minerals (Fig. 28).

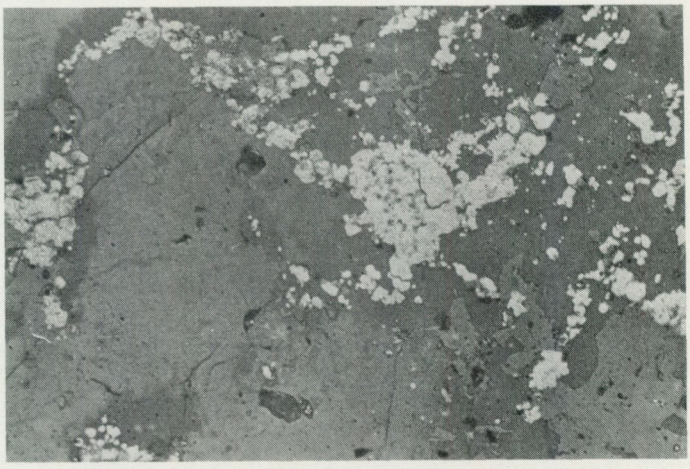

Fig. 28. Uraninite associated with skarn-like mobilisates inside the meta-chert. The silicates are darker grey on the microphoto. Note the inclusions of non-opaque minerals and white sulphides (galena?) in the uraninite. Reflected light, 240 x (Kå 102-2a/68).

2. NON-RADIOACTIVE ORE MINERALIZATIONS

2.1. GENERAL FEATURES OF MINERAL ASSEMBLAGES

Similarly to uraninite, the non-radioactive ore minerals are sparsely disseminated in the host rocks, only in places being gathered into thin layers which are conformable with the bedding of the enclosing rocks. The sparse disseminations also seem to have a general distribution which is conformable with the bedding of the host rocks. Almost exclusively, the mineralizations exhibit a banded structure. The grade of metal concentration is low. Four different mineral assemblages may be distinguished, each of them being associated with its own lithostratigraphic unit and connected with a special type of rock. An outline of occurring minerals is given in Fig. 29.

The four mineral assemblages have the following characteristics:

A s s e m b l a g e I occurs in the meta-basic lava (Bed 2) and is characterized by the predominance of magnetite. Copper is abundant in the form of chalcopyrite and bornite, the former dominating over the latter. Pyrite also occurs, but in small amounts.

A s s e m b l a g e II occurs in Bed 3. Here, pyrite is the dominant mineral, while uraninite and pyrrhotite are subordinate. The occurrence of small amounts of molybdenite is notable. Arsenopyrite is very rare. Magnetite is absent.

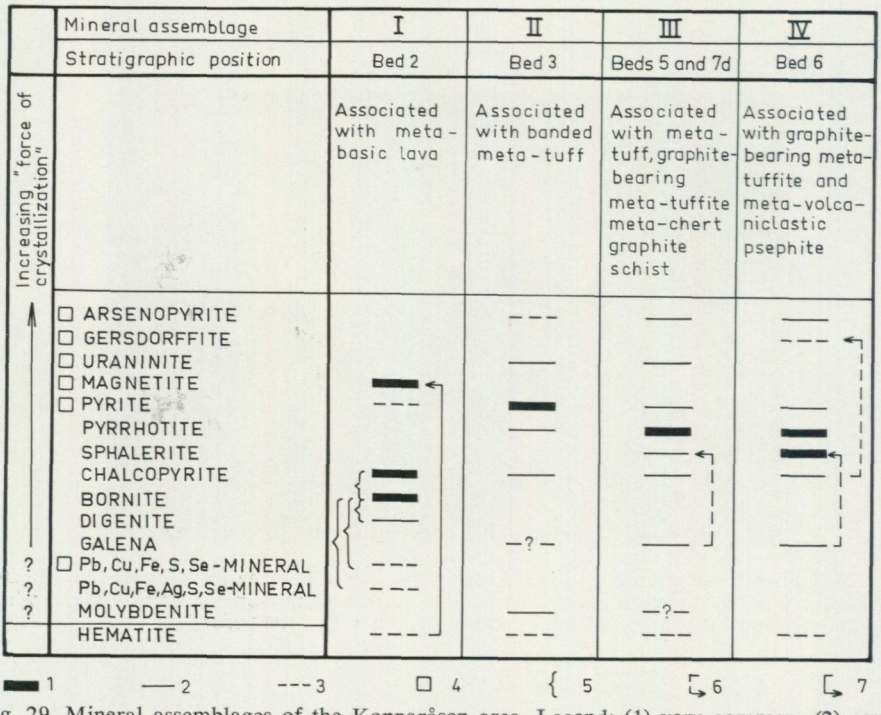

Fig. 29. Mineral assemblages of the Kopparåsen area. Legend: (1) very common, (2) common, (3) minor amounts, (4) occurs as euhedral crystals, (5) unmixture of solid solution, (6) texture resembling replacement, (7) replacement.

Assemblage III is associated with the graphite-bearing meta-tuffites, graphite schist and meta-chert of Bed 5 and Bed 7d. Pyrrhotite is the dominant iron sulphide. Pyrite is subordinate to pyrrhotite and in places also to sphalerite and chalcopyrite. Uraninite is common, but not dominant. Small amounts of arsenopyrite and galena also appears. Galena occurs in association with uraninite.

Assemblage IV is associated with graphite-bearing meta-tuffite which is interbedded in meta-volcaniclastic psephite (Bed 6) and rarely with meta-volcaniclastic psephite itself. Dominance of pyrrhotite and sphalerite. Chalcopyrite, pyrite, arsenopyrite and gersdorffite are subordinate. Galena is more common than in Bed 5, but still it is subordinate to pyrrhotite and sphalerite.

Minor pyrite and chalcopyrite mineralizations occur in Bed 14.

In spite of being "low-grade", the sulphide mineralizations occurring in Formation A may in many respects be directly compared with deposits of the "pyritic", "strata-bound" or "conformable" types. Mineralogical studies were therefore aimed to detect effects of their recrystallization caused by greenschist-grade metamorphism as well as to determination of their relationships with uranium mineralization. Criteria published recently by Stanton (1959, 1960, 1964) and Lawrence (1973) have been utilised for this purpose.

2.2. MINERALOGY OF THE NON-RADIOACTIVE ORE MINERALS

The intergrowths of opaque minerals, the intergrowths of opaque minerals with silicates and the apparent succession of minerals are identical in all the assemblages.

Concerning textural relationships of opaque to non-opaque minerals the following general osbervations have been made: All ore minerals contain inclusions of non-opaque minerals. Euhedral silicate inclusions appear within pyrrhotite, chalcopyrite, bornite, sphalerite and galena *but not in pyrite*. The inclusions are often rounded with sharp outlines. Euhedral crystals of ore minerals embedded in silicates are represented by arsenopyrite, gersdorffite, pyrite and rarely by magnetite and uraninite. Chalcopyrite, bornite, sphalerite and galena frequently appear as an infilling between grains of non-opaque minerals. There appears to be no sign of replacement of silicates by any of the ore minerals.

The ore minerals commonly display textural features which are characteristic for a metamorphic co-recrystallization. The observed textures were sorted into the three following groups:

1. Proper blastic textures (Figs. 30—38)
2. Exsolution textures (Figs. 39 a—c)
3. Textures resembling replacement (Figs. 40 a—c)

Examples of these textures are described below.

2.2.1. Intergrowths of other minerals with pyrite, representing proper blastic textures

Pyrite is one of the best suitable minerals for the study of blastic textures. It occurs in all assemblages and display different degrees of idiomorphism depending on the varying of external conditions more significantly than other minerals. In certain layers, pyrite occurs as equidimensional but anhedral grains while in other layers in the immediate neighbourhood, but of slightly different

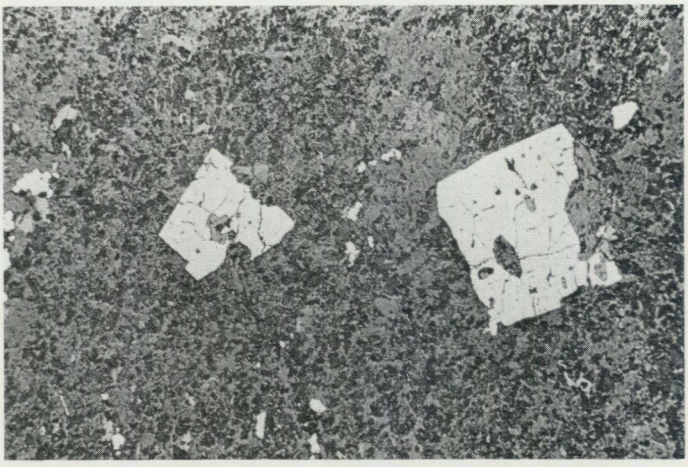

Fig. 30. Embayed megacrysts of pyrite in the banded meta-tuff. The elongated inclusions are arranged parallel to (100). Mineral assemblage II. Polished thin section. Reflected light, 120 x (Kå 31/68).

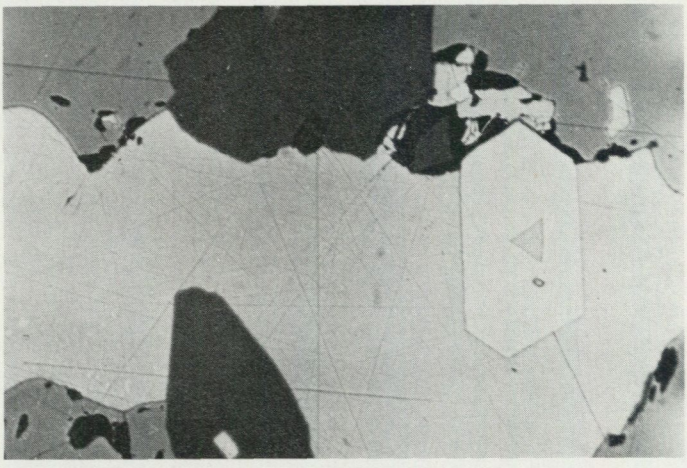

Fig. 31. Sharply euhedral pyrite surrounded by chalcopyrite which also occurs as inclusions inside the pyrite. It seems probable that the larger, triangular, inclusion is in fact a section of an embayment with pyrite crystal faces on its inside part. Magnetite is grey and amphibole dark grey. Mineral assemblage I. Reflected light, 240 x (Kå 179 B/69).

composition, it appears as cubes of differing perfection. Most frequently pyrite occurs as subhedral grains with individuals ranging from a few hundreds of a millimetre to about 3 mm. The best developed crystal faces are usually towards other sulphides, in contact with silicates pyrite crystals achieve sharp perfection more rarely. Very often, pyrite contains inclusions of other sulphides or non-opaque minerals. The inclusions are mostly rounded, elongated or nearly circular in section. Inclusions with outlines made up of pyrite crystal faces are rare. It is common that pyrite includes and is enclosed by one and the same mi-

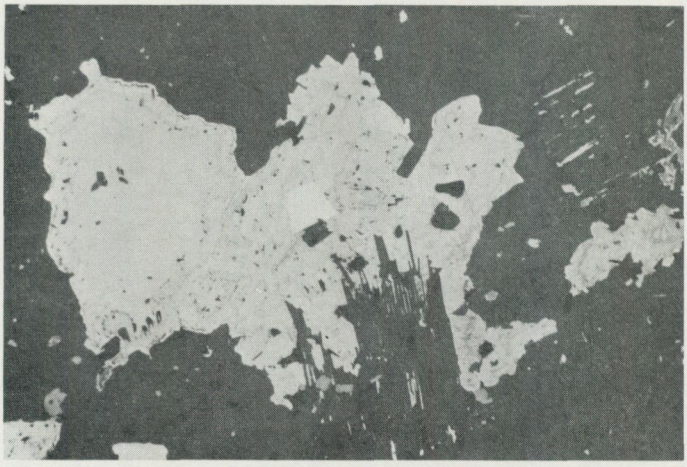

Fig. 32. Euhedral pyrite inside pyrrhotite and subhedral silicates in contact with partly oxidised pyrrhotite. Pyrrhotite mould about a mica and forms together with it helicitic-like aggregates. Mineral assemblage III. Reflected light, 120 x (Kå 265/69).

Fig. 33. Imperfect cubes of magnetite inside chalcopyrite. The inclusions inside magnetite consist of chalcopyrite and bornite. An example of a "poikiloblastic" texture of magnetite. Silicates are dark grey. Mineral assemblage I. Reflected light, 60 x (Kå 193/69).

Fig. 34. Typical blastic texture shown on the example of magnetite, bornite and amphibole intergrowths. Mineral assemblage I. Reflected light, 60 x (Kå 54/68).

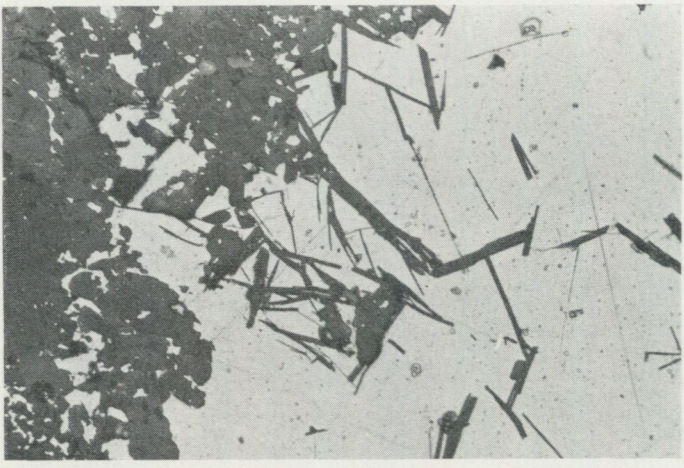

Fig. 35. Subhedral silicate laths included in galena. Galena moulds about the silicate and does not replace it. Mineral assemblage IV. Reflected light, 120 x (Kå 230/68).

neral. These "mutual inclusions" have been observed especially by the pairs pyrite-pyrrhotite and pyrite-chalcopyrite. Euhedral inclusions of opaque or non-opaque minerals have never been observed in pyrite. However, pyrite occurs as sharply euhedral single individuals included in pyrrhotite and chalcopyrite (Figs. 31 and 32).

Indentations or embayments of other minerals occur in abundance within the pyrite grains. They may form large "caries" which penetrate well into the centre of the crystals. Embayed crystals commonly contain elongated inclusions assorted mostly parallel with (100) planes (Fig. 30). Very rarely a development

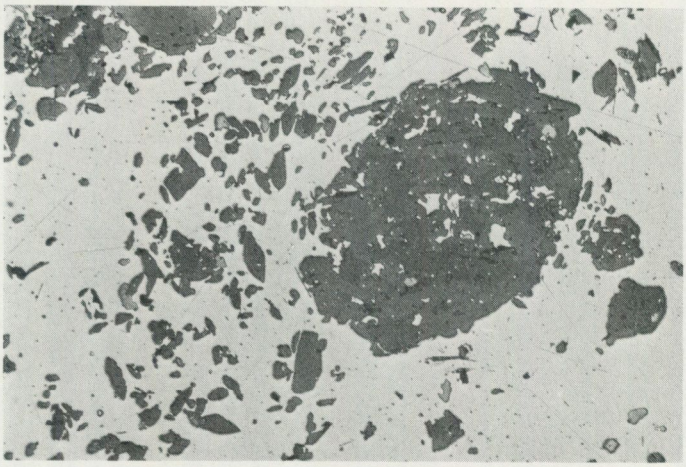

Fig. 36. Glomeroblastic aggregate of silicates within galena. Light grey minor phase is pyrrhotite. Note the roughly concentric arrangement of subhedral amphibole, included in galena. Mineral assemblage IV. Reflected light, 60 x (Kå 230/69).

Fig. 37. Molybdenite (showing reflection pleochroism) within meta-tuff. Mineral assemblage II. Reflected light, 120 x (Kå 28/68).

of pyrite crystal faces has been observed on the inside parts of the embayments (Fig. 31). These crystal faces are the main evidence against the dissolution hypothesis of Spry (1969) and support the theory that embayed crystals were formed by amoeboid growth or by coalescence.

It is apparent that the textural features of pyrite in the case considered, are the result of a very strong growth habit (of the pyrite) during the course of the greenschist metamorphism. Other intergrowths showing obvious recrystallization are presented in Figs. 33—38.

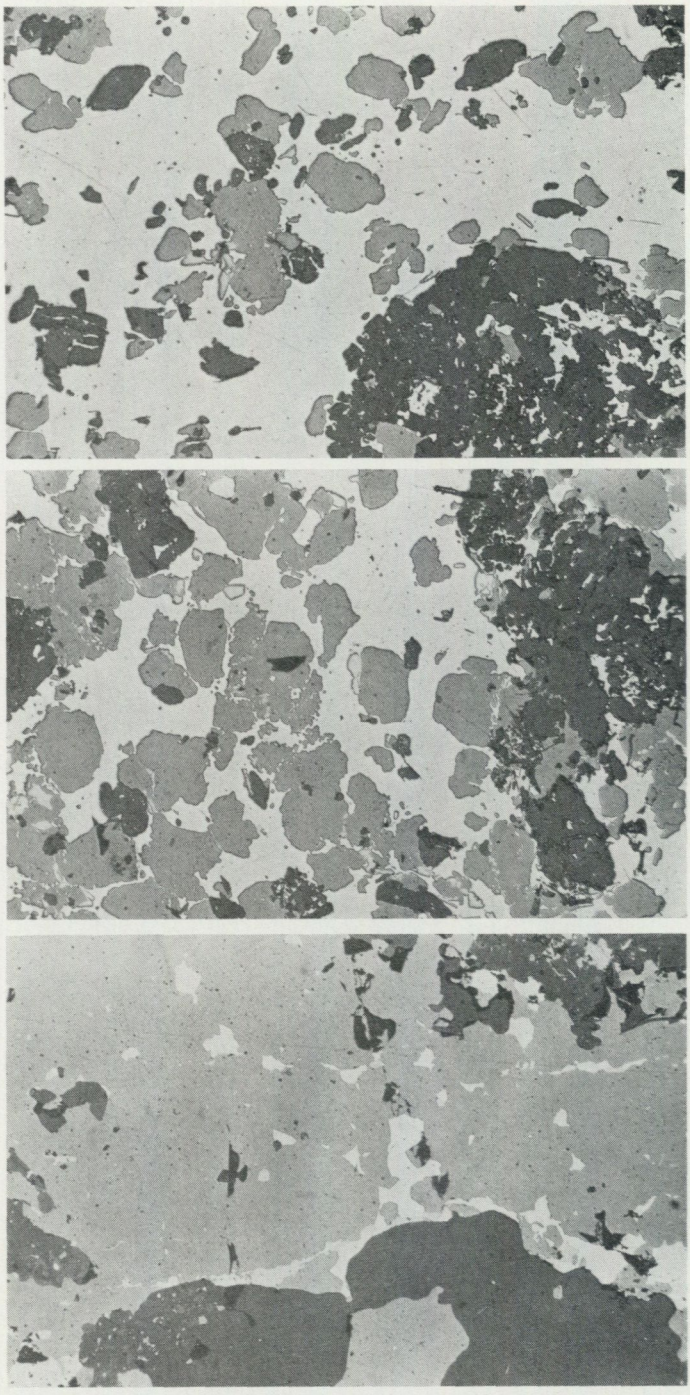

Figs. 38 a—c. Co-recrystallization of galena and sphalerite. Pyrrhotite is present as a minor phase. The silicates are dark grey.
a) Sphalerite, as a subordinate phase in galena, showing tendency to form rounded grains.
b) Sphalerite slightly dominates over galena. The early development of a cuspate form of galena. A mutual boundary texture is present as well.
c) Galena showing the cuspate form as a minor phase in sphalerite. The form of galena grains is controlled by triple point junctions and by grain boundaries of sphalerite. Mineral assemblage IV. Reflected light, a), b) — 60 x, c) — 120 x, (a, b: Kå 230/69, c: Kå 233/69).

2.2.2. Bornite, chalcopyrite and digenite intergrowths

Chalcopyrite, bornite and digenite are, with magnetite, the most common minerals in mineral assemblage I associated with the meta-basic lava. However, chalcopyrite appears only rarely together with bornite. If they appear together, bornite strongly dominates over chalcopyrite, and at the same time, digenite is absent. If bornite appears together with digenite, both minerals are in approximately equal proportions and display complicated intergrowths. Chalcopyrite is in these places mostly absent. (Chalcocite occurs as very fine, interstitial films within the bornite. The absence of any noticeable chalcocitisation in chalcopyrite is remarkable.)

B o r n i t e itself is anhedral, its outlines are subordinate to the habit of the silicates. In certain places, it moulds about the subhedral silicates, or the subhedral silicate laths are included in bornite. Frequently, bornite appears to be an intergranular filling between silicate crystal faces, and it does not replace them. Larger areas of chalcopyrite are apparent only on the boundary of bornite and the silicate. Chalcopyrite encroachs upon bornite as large embayments whose outlines are in general convex towards the bornite. In detail however, bornite and chalcopyrite exhibit vermicular intergrowths or mutual boundary texture at wide places along their boundaries. In specimens with fairly large areas of chalcopyrite, many fine blebs or shreds of bornite are included in the chalcopyrite (Figs. 39a and b).

A very different type of intergrowth is represented by the crystallographically oriented thin lamellae, flame-like bands and wedges of chalcopyrite which mostly appear at the periphery of bornite grains but also in the central part of them (Figs. 39b and c). The boundaries of the blades are sharp and smooth. The lamellae are narrower when they intersect or meet each other. Well developed lattice work of chalcopyrite occurs very rarely within bornite grains which are completely surrounded by magnetite. Chalcopyrite almost exclusively makes up minute veinlets penetrating magnetite. These veinlets, however, have never been observed in sulphides.

Taking into account the existence of the blastic texture of bornite and coexisting minerals such as magnetite, pyrite etc., there is little doubt that all described intergrowths of chalcopyrite and bornite represent the unmixing of a solid solution. Similar textures have been described by e. g. Geijer (1923), Schwarz (1931), Sugaki (1955) and Brett (1964).

The same bornite grains which carry the flame-like inclusions of chalcopyrite contain in places fine euhedral laths (0.02—0.03 mm) and larger irregular blebs (up to 0.08 mm) of a white isotropic mineral. The laths mostly occur in a regular pattern in obvious relation to grain boundaries or crystallographical directions of the bornite. Some of the larger blebs are composed of two mineral phases. In addition to the white isotropic mineral, there appears another mineral which is anisotropic and with pronounced reflection pleochroism — very pale grey/

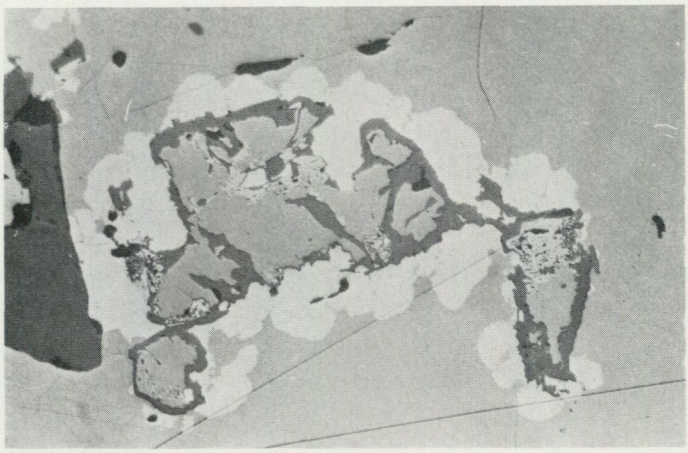

Fig. 39 a. "Rim texture" resulting from the unmixing of a chalcopyrite-bornite solid solution, with subsequent segregation of unmixed chalcopyrite in the grain boundaries of the bornite and titanite (darker grey) which envelops magnetite. Magnetite is partly hematitised. Note that hematite does not show any sign of a recrystallization. Hematitisation is in general very rare. Mineral assemblage I. Reflected light, 60 x Kå 179 A/68).

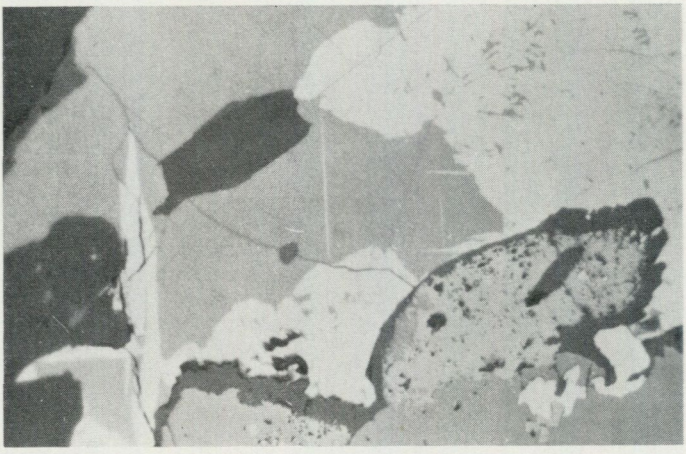

Fig. 39 b. Exsolution intergrowths of blades of chalcopyrite in the crystallographic planes of bornite and fine blebs of bornite in chalcopyrite. Mineral assemblage I. Reflected light, 240 x (Kå 179 A/68).

greenish blue. Both minerals have been analysed in the Chemical Laboratory of the Geological Survey of Sweden by use of the energy dispersive spectrometry. The white isotropic mineral contains Pb, Se, Cu, Fe and S in approximate proportions equal to 5:1:1:1:1. The anisotropic mineral contains Pb, Se, Cu, Fe, Ag and S. Silver is present in roughly the same amount as Cu and Fe. The contents of Pb and S are lower than those of the first mineral[1].

[1] Chemical "whole rock" analyses of samples of mineral assemblage I exhibit strong positive correlation of Ag and Cu along with high relative abundance of Ag (Fig. 42).

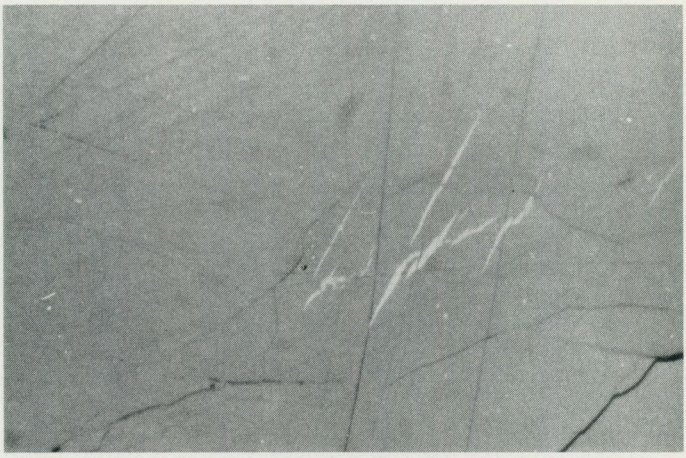

Fig. 39 c. Exsolution intergrowth of the flame-like bands in the central part of the bornite grain. Mineral assemblage I. Reflected light, 600 x (Kå 179 A/68).

D i g e n i t e[2], where present, is intricately intergrown with bornite. Among the observed microtextures the so-called sub-graphic or pseudo-eutectic seems to be the most common. However, so much controversy has arisen regarding the possible origin and interpretation that these textures themselves cannot be used with confidence as criteria for any particular origin.

To understand the final conclusion concerning the interpretation of the observed chalcopyrite-bornite-digenite intergrowths, it is necessary to mention results of some foregoing studied. Sales and Meyer (1951) demonstrated, that the pyrite-chalcocite assemblage of Butte's Central zone transformed to chalcopyrite-bornite as a consequence of the thermal metamorphism. Where chalcocite was silver-bearing, native silver was exsolved in the reaction. The assemblage with enargite was transformed to chalcopyrite-bornite-tennantite. The authors have evidence in their paper for suggesting that all the textures, geometrically suggestive of replacement of bornite by chalcopyrite, can be generated in the solid state by exsolution and minor subsequent recrystallization. The experimental work of Brett (1964) shows that this conclusion is correct. Chalcopyrite lamellae within bornite formed by thermal metamorphism have also been described by Filimonova (1959), who was able to form in the laboratory chalcopyrite from bornite and pyrite by heating in an open system with a low partial pressure of sulphur. The chalcopyrite formed textures similar to those observed in the case studied.

The microscope study results of Cu-Fe-S minerals from the Kopparåsen area coupled with the results of previous workers allow the pressumption that all textures discerned by the above mentioned minerals were generated in conse-

[2] The present digenite was defined in the Laboratory of Geological Survey of Sweden. See appendix.

quence of the greenschist metamorphism. There is no evidence that a pyrite phase took part in the formation of chalcopyrite or bornite. However, the special features of the distribution of bornite, digenite and chalcopyrite suggest some modifications in the Cu-Fe-S mineral system, depending on the metamorphism.

2.2.3. Textures resembling replacement

Among all the observed minerals, the pair gersdorffite-chalcopyrite suggests most expressively a texture resembling replacement, viz. replacement of gersdorffite by chalcopyrite (Fig. 40). Gersdorffite itself shows a strong tendency to idiomor-

Fig. 40 a. Intergrowths of gersdorffite (white) with chalcopyrite. Mineral assemblage IV. (Kå 248/69). General view. Reflected light, 60 x.

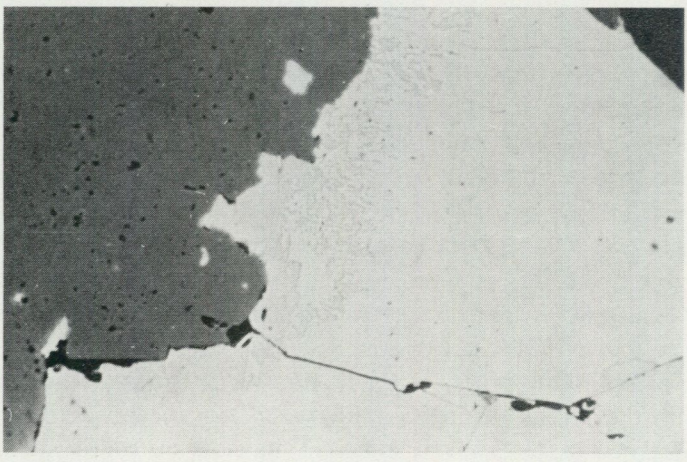

Fig. 40 b. Intergrowths of gersdorffite (white) with chalcopyrite. Mineral assemblage IV. (Kå 248/69). Vermicular intergrowths of chalcopyrite and gersdorffite along the crystal boundary of gersdorffite. Reflected light, 240 x.

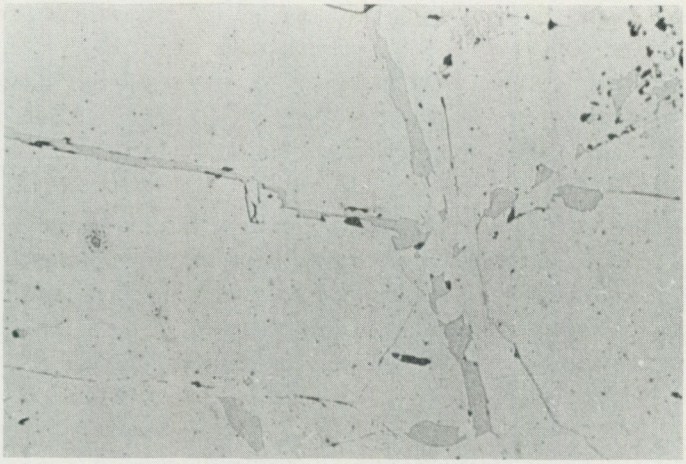

Fig. 40 c. Intergrowths of gersdorffite (white) with chalcopyrite. Mineral assemblage IV. (Kå 248/69). Chalcopyrite veining gersdorffite along (210) planes. Note that the chalcopyrite veins disappear before meeting at an intersection point. Reflected light, 240 x.

phism, more so than pyrite. Its crystal faces are broken by arsenopyrite crystalloblasts. When in contact with chalcopyrite, the crystal outlines of gersdorffite are sharp in places, but frequently, chalcopyrite intergrows with the gersdorffite forming a vermicular texture. Chalcopyrite also penetrates gersdorffite in the form of veins with nonmatching borders of walls (Fig. 40c). These veins are often composed of short disjointed segments and have an obvious relationship to the crystallographic directions of gersdorffite. Development of gersdorffite crystal faces can be observed on the inside walls of the veins. It seems also characteristic that two concurrent chalcopyrite veins disappear just before meeting at an intersection point (Fig. 40c). The intergrowth described seems likely to represent a "locked inclusion" rather than replacement texture. The texture illustrated in Fig. 40b is more problematic. The gersdorffite is corroded by chalcopyrite over large areas along grain boundaries where a fine vermicular intergrowth develops. Similar textures of a recrystallized ore are mentioned by Lawrence (1973).

The observed chalcopyrite-gersdorffite intergrowths demonstrate the complex nature of the metamorphic recrystallization. They indicate a coalescence and metamorphic mobilization rather than a simple replacement.

3. SOME REMARKS ON THE GEOCHEMISTRY OF THE URANIUM MINERALIZATIONS

No systematic geochemical investigation has been undertaken and these comments are based exclusively on analyses made on samples which were taken in the course of the prospecting work. At the outcrops, samples were taken from

the parts with highest radioactivity or from the parts apparently rich in sulphide minerals.

From drill-cores, samples were taken of intervals exhibiting anomalous radioactivity as demonstrated by the help of gamma-logging in the holes or scanning of the drill-cores. Thus, no analyses to establish the geochemical background have been made.

The analyses of non-radioactive elements were performed by the Geochemical Laboratory of SGU, the analyses of U and Th by the Laboratory of Industrins vatten- och luftvård AB. All samples were crushed and ground and one part of each sample was buffered and quantitatively analysed for the following elements with the help of a direct-reading optical spectrometer (Danielsson 1968): Cu, Pb, Zn, Sn, Bi, Ag, Mo, As, Fe, Mg, Ti, Ca, Mn, Ba, V, Sr, Co, W, Ni. U was determined fluorimetrically (Centanni et al., 1956), Th spectrophotometrically.

A simple statistical analysis was used to resolve the intercorrelation of U and Cu, Pb, Zn, Bi, Ag, Mo, As, Fe, Ti, Ca, V, Co and Ni. (The contents of Th are always lower than the lower sensitivity limit which, for the analytical method used, is 0.002 % Th.) The statistical results of raw and $\log_{10}$ transformed data are given in Table 2. Because of the unsatisfactory number of samples only highly significant relationships can be considered.

In the data set of mineral assemblage II (23 samples), uranium shows positive correlation at the significance level >95 % only with Pb and As, moreover the correlation strength of these relationships is quite low. The surprisingly weak correlation between Pb and U can be explained through the extensive uranium mobilization which was also established by the mineralogical studies (see chapter IV). Pb itself is correlated with Ag, Fe, Co, V, Ni, As, Zn and Cu (the elements are listed in order of decreasing correlation strength). As, which is present as rare arsenopyrite, is correlated with Pb, Ag, V and Mo (the correlation with Mo is weak). Taking into account the above described relationships, it seems that uranium's element association includes, in addition to Pb and As, also V which shows weaker correlation with U (coef. cor. = 0.33, probability for this coefficient is 0.94). As vanadium is correlated with Cu, Pb, Ag and As, it is not impossible that vanadium is also present as a sulphide accompanying other sulphides and uraninite. The last element, which could belong to this association is Mo. Molybdenum shows weak correlation with U (coef.cor. = 0.27, probability for this coefficient is only 0.89) and Bi, Ag, As. However, a relatively high mean for Mo in the studied data set is notable. Mo is present as molybdenite.

From mineral assemblage III, only 15 sampels analysed for uranium are available. In this data set U is correlated with Pb, Ag, Co, As, Bi, Fe and Cu (the elements are listed in order of decreasing correlation strength, significance level is >95 %). This association includes probably also Zn as this element is correlated with Pb, Co and Fe, but the correlation with U is weak and less significant (coef.cor. = 0.32, probability for this coefficient is 0.88). Distribu-

TABLE 2. Statistical data, samples with uranium content >100 ppm U

	Mineral assemblage II, 23 samples					Mineral assemblage III, 15 samples				
	Mean	Std.dev.	Mean ($\overline{X}$ log)	Std.dev.	G (antilog $\overline{X}$ log)	Mean	Std.dev.	Mean ($\overline{X}$ log)	Std.dev.	G (antilog $\overline{X}$ log)
U	468	451	2.543	0.315	349	864	1269	2.699	0.433	499
Cu	308	211	2.384	0.329	242	226	184	2.278	0.245	189
Pb	210	119	2.255	0.255	179	305	579	2.254	0.338	179
Zn	261	163	2.359	0.217	228	186	110	2.227	0.182	168
Bi	6	9	0.463	0.468	2	2	2	0.224	0.358	1
Ag	1.4	1.4	— 0.109	0.607	0.7	2.8	8.0	— 0.093	0.552	0.8
Mo	198	184	2.043	0.570	110	260	191	2.344	0.250	220
As	12	14	0.912	0.352	8	162	372	1.490	0.833	30
Σ Fe as Fe_2O_3	8.0	3.3	0.871	0.173	7.4	13.3	7.7	1.084	0.179	12.1
TiO_2	1.10	0.5	— 0.002	0.198	0.99	0.97	0.34	— 0.041	0.180	0.90
CaO	5.7	3.13	0.704	0.212	5.0	6.8	1.5	0.825	0.112	6.6
V	908	366	2.923	0.181	837	1179	249	3.063	0.092	1154
Co	31	16	1.453	0.206	28	63	61	1.702	0.271	50
Ni	140	53	2.119	0.162	131	293	105	2.439	0.174	275

Values in ppm, Fe_2O_3, TiO_2, CaO in %.

TABLE 3. Statistical data, mineral assemblages II, III and skarn-like mobilisates. 57 samples with uranium content >100 ppm U

	Mean	St.dev.	Mean ($\overline{X}$ log)	St.dev.	G (antilog $\overline{X}$ log)	clarke			$\overline{X}$ expressed as concentration clarkes	G expressed as concentration clarkes
U	486	753	2.419	0.514	262	3.6	ppm	(K)	135.00	72.77
Cu	530	2261	2.237	0.471	172	55	ppm	(M)	9.63	3.12
Pb	304	514	2.224	0.418	167	13	ppm	(M)	23.38	12.84
Zn	378	761	2.384	0.331	242	70	ppm	(M)	5.40	3.45
Bi	3.7	6.7	0.344	0.399	2.2	0.2	ppm	(M)	18.50	11.00
Ag	2.0	5.1	— 0.068	0.537	0.8	0.07	ppm	(M)	28.50	11.42
Mo	159	177	1.851	0.668	71	1.5	ppm	(M)	106.00	47.33
As	68	203	1.319	0.631	20	1.8	ppm	(M)	37.77	11.11
Fe	8.6	5.9	0.854	0.273	7.1	5.0	%	(M)	1.72	1.42
Ti	0.85	0.67	— 0.409	0.760	0.39	0.44	%	(M)	1.93	0.88
Ca	6.3	2.9	0.766	0.192	5.8	3.63	%	(M)	1.73	1.59
V	1651	1597	3.038	0.497	1090	135	ppm	(M)	12.22	8.07
Co	49	110	1.472	0.355	29	25	ppm	(M)	1.96	1.16
Ni	164	118	2.103	0.330	126	75	ppm	(M)	2.18	1.70

(K) L. V. Komlev, in Basic principles of the uranium geochemistry, A. P. Vinogradov (Editor), Moskva 1968 (in Russian).
(M) B. Mason, Principles of geochemistry. New York 1966.

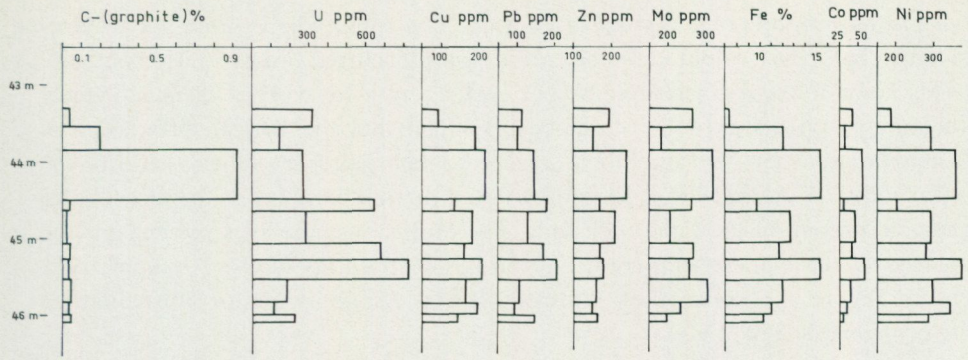

Fig. 41. The variation of C, U, Cu, Pb, Zn, Mo, Fe, Co and Ni in drill-core no. Kå-69007 with respect to the sample depth. Mineral assemblage III.

tion of graphite and U, Cu, Pb, Zn, Mo, Fe, Co, Ni in the drill-core from the mineralized section in Bed 5 is shown in Fig. 41. It has been mentioned that uranium mineralizations are in Beds 5 and 7d associated with graphite-bearing rocks. However the analysed samples exhibit no obvious correlation between U and C (graphite).

A comparison of the untransformed and transformed mean values of the whole data set (57 samples, skarn-like mobilisates included) with the mean crustal abundance of the element is shown in Table 3. As is seen, U and Mo display the greatest divergence from the mean abundance, accentuating the position of uranium as being the most important element of the mineralizations studied.

IV. DISCUSSIONS AND CONCLUSIONS

The important parts of the uranium mineralizations occur in Bed 3 and Bed 5 where they compose, together with sulphide minerals, the characteristic assemblages of ore minerals. The uraninite and sulphides are gathered into seams which are perfectly conformable with the bedding of the host rocks, even in those parts, where the bedding was disturbed by a synsedimentary subaquatic slumping (Fig. 18). In Bed 3, the host rocks are represented by meta-tuffs, in Bed 5, by graphite-bearing meta-tuffite.

No direct correlation between uranium and graphite can be distinguished (Figs. 21 and 41).

One of the striking features of the host rocks, and of the all rocks in the area studied, is an abundance of preserved original structures and mineral relicts indicating low stresses associated with the metamorphism. The characteristic mineral assemblages produced by this metamorphism are not critical for any particular mineral subfacies. Biotite and amphibole dominate strongly over chlorite, but the pair epidote/albite characterize the greenschist facies. Newly formed

plagioclase in the range above An_{15} is rare. The amphibole is often green hornblende, but a pale-coloured or colourless, non-pleochroic variety is also common. This has a lower extinction angle (21—24°) and a lower birefrigence. Typical actinolite appears as well. It can be presumed that the optical differences of amphiboles, when the amphibole grains do not represent relicts, reflects the availability of Al and Fe. It should be noted that all varieties of the amphiboles may be present in the same rock slice. The mineral assemblages present may be placed in the highest temperature green-schist subfacies of the Abukuma-type according to the concept of Winkler (1967). Its upper temperature limit is approximately 550° C.

The textures of the sulphide minerals, magnetite and uraninite which constitute the mineral assemblages of the Kopparåsen area were interpreted with the help of criteria published by Stanton (1959, 1960, 1964) and Lawrence (1973). A metamorphic mode of origin, i. e. metablastic growth, seems the most probable. According to the relative tendency to idiomorphism reflecting their "force of crystallization" towards surrounding minerals, the ore minerals may be placed in a sequence, which is similar to the crystalloblastic series proposed by Stanton (1.c.). The established sequence is as follows:
arsenopyrite, gersdorffite — uraninite, magnetite, pyrite — pyrrhotite — sphalerite — chalcopyrite, bornite, digenite — galena.

The position of molybdenite, and unidentified minerals of Pb, Cu, Fe, Ag, S, Se is rather uncertain. Textures as a consequence of unmixing from a solid solution are rather common and represent perhaps a characteristic feature of the metamorphosed ores. The blastic textures of the ore minerals could be taken as evidence for premetamorphic origin of the ore mineralization.

Evidence for the contemporaneous deposition of uranium and the host rock are (*1*) association of the main part of the uranium mineralizations with special lithostratigraphic units, (*2*) "sedimentary" structures of the strata-bound bodies, thoroughly conformable with the preserved internal structures of the host rock, (*3*) occurrence of uraninite-bearing fragments embedded in the meta-tuff of Bed 5, which also shows, that a partial reworking took place during the deposition.

Taking for granted that the ore minerals are an integral part of the rocks in which they occur, their intergrowths must also reflect the pressure-temperature conditions of the metamorphism. Many attempts were made to use Cu-Fe-S minerals as geothermometers but it is now generally accepted that the use of them is not as straightforward as was previously thought. The relationship of the minerals of the ternary system Fe-As-S, which occur in the assemblages II, III and IV, to metamorphic conditions seems more unambiguous. The data published by Clark (1960) show that the temperature limitation for the co-existence of the mineral pair pyrite-arsenopyrite is 491 $\pm 12°$ C, and 528 $\pm 10°$ C respectively at a confining pressure of 2 070 bars.

No evidence for the mobilisation of the sulphide minerals, extending over the volume of the proper ore aggregates has been established. However, the character of the uranium occurrence allows a multiphase mobilization of uranium to be assumed.

Two general types of uraninite textures may be distinguished:

a. The proper blastic texture appropriated to uraninite grains scattered in the mineralised seams (Figs. 23 and 25). The uraninite adopts a rather varying degree of idiomorphism owing to different external conditions. The cubes of uraninite display the highest degree of idiomorphism, and irregular and rounded grains the lowest. Compared with the other ore minerals in contact with uraninite — pyrite, pyrrhotite and galena show a lower tendency to idiomorphism than uraninite, while arsenopyrite shows a higher tendency.

b. Mobilisation texture. Uraninite exhibits a pronounced tendency to concentrate in thin laminae or string-like aggregates. These aggregates follow in general the bedding of the host rock. In banded meta-tuffs, they occur on the boundaries between dark and light beds, but they also cut the individual beds. Uraninite gathered in the laminar aggregates shows in general lower degree of idiomorphism than uraninite scattered in the host rock. Fluorite has been observed close to the uraninite aggregates, but not directly in contact with uraninite. In Bed 3, the schlieren-like aggregates, which are made up of hornblende, intersect the laminar aggregates of uraninite. On the other hand, some of the string-like aggregates of uraninite intersect the scapolite porphyroblasts in Bed 5.

The uraninite is also associated with skarn-like bodies related to regional metamorphism and occur in small veinlets associated with minor faults and joints. Fluorite also appears in the skarn-like mobilisates, but it has never been observed in direct contact with the uraninite. The uraninite occurs here only in the anhedral form.

The heterogeneity of the uraninite occurrence is apparently due to a redistribution of uranium during the course of the greenschist metamorphism and subsequent metasomatic processes. As scapolite is assumed to be connected with a granitization, the possibility of a uranium mobilisation generated by granitization processes can not be wholly eliminated. However, no observations pointing in this direction were made during the field work.

Uraninite (s.l.) textures, interpreted as a result of metamorphism, have been described in the previous literature only from Alpine deposits (Cevales 1960, 1961). Although the character of metamorphism was rather different there (dynamothermal metamorphism of low rank), Cevales has been able to distinguish the multi-phase mobilisation of the uranium oxide which resulted in the separation of discrete grains of the botryoidal pitchblende. The pitchblende grains are disseminated in the host rock and in places are gathered into string-like aggregates. The crystallization temperature of pitchblende was low, approximately

150—250° C. No development of uraninite crystalloblasts was observed though pyrite, occurring together with pitchblende, recrystallized from the original "pyrite bacterium" to sharply euhedral crystals. Nevertheless, Cevales (l.c.) brings corroborative evidence for contemporaneous, crystallization of pyrite and pitchblende. Blastic and mobilisation textures of uraninite are likely to occur in many deposits but their identification seems to be rather difficult due to the absence of large amounts of sulphide minerals. For example some of the uranium textures from the Koli-Kaltimo district in Finland (Piirainen 1968) strongly resemble textures generated by metamorphism.

The mobilisation of uranium in the case studied has been established by the use of "purely" geological methods and confirmed, at least to a certain degree, statistically. As regards the mobilisation process itself, it is suggested that uraninite was on one hand separated from the host rocks, and on the other, subsequently moved relative to the enclosing rocks. The only process which can explain this is a fluid phase transport, however, this implies many problems. As it is known (see e. g. Vinogradov 1963), uranium transforms into compounds which readily dissociate in water solutions and form U^{4+} ions only in an extremely acidic medium. In neutral environments, the concentration of U^{4+} ions is extremely small. On the other hand, hydrolysis of the uranyl ion does not require such rigorous limits (the concentration of UO_2^{2+} ions can reach up to 3.2×10^{-5} g/l by pH = 8) however, the uranyl ion is easily reduced into an insoluble four-valent form. Solutions passing through the rock complex containing abundant reducing agents such as sulphides and graphite were obviously not endowed with a high oxidation potential and the concentration of the uranyl ion was probably extremely low in them. Nevertheless, the rarely occurring hematitisation of magnetite indicates the attendance of oxidising water or water vapour, evidently in a postmetamorphic stage as pyrrhotite is preserved and hematite does not bear any traces of a recrystallization.

However, the most probable form for uranium transfer during the mobilisation seems to be as complex ions — uranyl carbonate, uranyl fluoride or mixed uranyl fluoride carbonate. These complexes are stable even at higher temperatures, and low values of their redox potentials allow for their occurrence in the equilibrium with a whole range of natural reducing agents. The experimental work of Naumov (1962) confirmed that under an excess of CO_3^{2-} ions, U^{6+} which is bounded in $[UO_2(CO_3)_3]^{4-}$ will not be reduced into U^{4+} not even by means of sulphidic sulphur. Uranyl fluoride ion complexes are important for uranium transfer only under the condition that the concentration $[F^-] \gg [CO_3^{2-}]$. The maximal development of uranyl fluoride ion complexes is in an acid milieu.

Occurrences of the carbonates and fluoride close to the laminar mobilisates of uraninite indicate that uranyl complex ions could have assisted the uranium mobilisation in the case studied. The mobilisation of uranium associated with a formation of skarn-like bodies has probably a different character and occurs

under different conditions than mobilisation connected with the formation of laminar uraninite aggregates. As the experimental data concerning the behaviour of uranium in metamorphic processes is lacking, the author is not in a position to throw more light on the chemical processes involved in the mobilisation.

The Kopparåsen occurrence represents a rather unusual type of uranium mineralization, with many features unknown from other places. Unfortunately, lack of special investigation does not permit any conclusions to be made concerning a mode for the primary uranium transfer and the character of the uranium source. However, the observed relationships strongly substantiate (1) *a pre-metamorphic, most likely volcanic-sedimentary origin for the uranium and sulphide mineralizations, (2) a multiphase mobilisation of uranium, generated by greenschist-grade metamorphism and subsequent endogenous processes.*

ACKNOWLEDGEMENTS

The Kopparåsen uranium project started in the summer of 1968 and I wish before anything else to extend my gratitude to Dr. B. Lundberg, G. Åkerblom, R. Kumpulainen and T. Lager who in the cold and rainy August of 1968 took part in the field investigations and who supported me with their friendship while I was sometimes run down. The field work continued with Dr. S. Hammarbäck, B. Gustavsson and H. E. Lundgren in the summer of 1969. These and all others who participiated in the Kopparåsen project are thanked for their contributions.

Thanks are due to Dr. G. Kautsky, Dr. B. Lundberg, Dr. M. Ambros, Dr. O. Brotzen and Dr. G. Juve for their critical reading of the manuscript. I am also indebted to Mrs. I. Schenling who drew the maps and figures, to Dr. A. M. Byström-Brusewitz for her help with mineralogical analyses and to Mrs. C. Wilson for correcting the English of the manuscript.

Miss E. Månsson kindly undertook the typewriting of the manuscript.

REFERENCES

GFF = Geologiska Föreningens i Stockholm Förhandlingar
SGU = Sveriges geologiska undersökning

ADAMEK, P. M., 1973: Kopparåsen Uranium Project. Results of prospection work carried out during the years 1968—1970. — SGU, unpublished report.

BOUŠKA, V., 1968: On the original rock source of tektites. — Lithos 1, 102—112.

BRETT, R., 1964: Experimental data from the system Cu-Fe-S and their bearing on exsolution textures in ores. — Econ. Geol. 59, 1241—1269.

CENTANNI, F. A., ROSS, A. M., DESESA, M. A., 1956: Fluorometric determination of uranium. — Analytical Chemistry 28, 1651—1657.

CEVALES, G., 1960: Erzmikroskopische Untersuchung von zehn Uranvorkommen des italiennischen Perms der West- und Ostalpen. — N. Jahrb. Mineral. Abhandl. 94, 733—758.

— 1961: Metamorphe Mobilisationvorgänge in der Uranlagerstätte des Preittals (Kottische Alpen). — N. Jahrb. Mineral. Abhandl. 96, 112—123.

CLARK, L. A., 1960: The Fe-As-S system. Phase relations and applications. — Econ. Geol. 55, 1345—1381, 1631—1652.

DANIELSSON, A., 1968: Spectrochemical analysis for geochemical purposes. — In XIII Colloquium spectroscopicum internationale, Ottawa (Hilger, London), 311—323.

ERIKSSON, B., (in print): Beskrivning till berggrundskartbladen Vittangi NV, NO, SV, SO. — SGU Af 13—16.
FILIMONOVA, A. A., 1959: Textures due to unmixing of solid solutions in ores alterated by metamorphism (in Russian). — Geologija Rudnych Mestorožděnij 1, 81—88.
FISHER, R. V., 1961: Proposed classification of volcaniclastic sediments and rocks. — Bull. Geol. Soc. Am. 72, 1409—1414.
— 1966: Rocks composed of volcanic fragments and their classification. — Eearth- Sci. Rev. 1, 287—298.
GEIJER, P., 1924: Some Swedish occurrences of Bornite and Chalcocite. — SGU C 321, Årsbok 17.
— 1931: Berggrunden inom malmtrakten Kiruna-Gällivare-Pajala. — SGU C 366.
GREEN, J., SHORT, N. M. (editors), 1972: Volcanic landforms and surface features. New York.
GRIP, E., FRIETSCH, R., 1973: Malm i Sverige 2. — Almqvist & Wiksell, Stockholm.
HOLMQVIST, P. I., 1910: Die Hochgebirgsbildungen am Torne Träsk in Lappland. — GFF 32, 913—983.
KÖHLER, A., RAAZ, F., 1951: Über eine neue Berechnung und graphishe Darstellung von Gesteinsanalysen. — N. Jahrb. Mineral. Monatshefte, 247—263.
KULLING, O., 1964: Översikt över norra Norrbottensfjällens kaledonberggrund. — SGU Ba 19.
LAWRENCE, L. J., 1973: Polymetamorphism of the sulphide ores of Broken Hill, N. S. W., Australia. — Mineral. Deposita 8, 211—236.
NAUMOV, G. B., 1962: Synthesis and decomposition of pitchblende in the carbonate-bearing medium (in Russian). — Trudy VI. Soveščanija po eksp. min. i petrogr. Izd.-vo AN SSSR, Moskva.
OFFERBERG, J., 1967: Beskrivning till berggrundskartbladen Kiruna NV, NO, SV, SO. — SGU Af 1—4.
PADGET, P., 1970: Beskrivning till berggrundskartbladen Tärendö NV, NO, SV, SO. — SGU Af 5—8.
PETERSSON, W., 1897: Om de geologiska förhållandena i trakten omkring Sjangeli koppar-malmsfält i Norrbottens län. — SGU C 171, 1—13.
PIIRAINEN, T., 1968: Die Petrologie und die Uranlagerstätten des Koli — Kaltimogebietes im finnischen Nordkarelien. — Bull. de la Comm. Géol. de Finlande 237, 1—99.
RAMDOHR, P., 1969: The ore minerals and their intergrowths. — Pergamon Press, Oxford, etc.
SALES, R. H., MEYER, CH., 1951: Effect of post-ore dike intrusion on Butte ore minerals. — Econ. Geol. 46, 813—820.
SCHWARTZ, G. M., 1931: Intergrowths of bornite and chalcopyrite. — Econ. Geol. 26, 186—201.
SPRY, A., 1969: Metamorphic textures. — Pergamon Press, Oxford, etc.
STANTON, R. L., 1959: Mineralogical Features and possible mode of emplacement of the Brunswick mining and smelting orebodies, Gloucester County, New Brunswick. — Canadian Min. and Met. Bull. 52, 631—642.
— 1960: General features of the conformable "pyritic" orebodies. Part II. — Canadian Min. and Met. Bull. 53, 66—74.
— 1964: Mineral interfaces in stratiform ores. — Trans. Inst. of Min. and Met. 74, 45—79.
SUGAKI, A., 1955: Thermal studies on the lattice intergrowth of chalcopyrite in bornite from the Iinmu mine, Japan. — Sci. Repts. Tohoku Univ., Ser. III., 5, 113—128.
TEGENGREN, F. R., 1924: Sveriges ädlare malmer och bergverk. — SGU Ca 17.
VINOGRADOV, A. P. (editor), 1963: Basic principles of the uranium geochemistry (in Russian). — Izd-vo AN SSSR, Moskva.
WINKLER, H. G. F., 1967: Petrogenesis of metamorphic rocks. — Springer-Verlag, Berlin, etc.
ÖDMAN, O. H., 1957: Beskrivning till berggrundskarta över urberget i Norrbottens län. — SGU Ca 41.

TABLE 4a. Chemical analyses of uranium-bearing banded meta-tuffs from Bed 3

Analysis 001: Sample	3420 KÅC 1	3421 KÅC 2	3422 KÅC 3	3423 KÅC 4	3414 KÅC 5	3415 KÅC 6	Average
SiO_2	49.6	60.2	50.9	60.9	54.3	54.9	55.1
TiO_2	0.82	0.65	0.58	0.72	0.70	0.74	0.70
Al_2O_3	15.2	15.0	10.1	14.1	14.3	15.2	13.9
Fe_2O_3	5.8	4.1	7.6	1.8	3.8	4.2	4.5
FeO	7.4	3.8	8.9	8.1	8.9	6.8	7.3
MnO	0.35	0.12	0.38	0.08	0.18	0.21	0.22
CaO	5.8	3.7	9.6	2.1	3.6	4.7	4.9
MgO	6.2	3.8	6.6	3.3	5.1	4.2	4.8
Na_2O	2.0	3.9	0.6	3.1	2.8	3.8	2.7
K_2O	3.1	2.7	1.5	3.0	3.5	2.4	2.7
H_2O >105°	2.4	1.7	2.5	1.5	1.6	1.7	1.9
H_2O <105°	0.4	0.3	0.5	0.2	0.2	0.2	0.3
CO_2	0.06	0.09	0.02	0.01	0.22	0.19	0.09
F	0.48	0.20	0.16	0.17	0.41	0.46	0.31
S	0.79	0.54	1.2	2.0	0.53	0.62	0.94
BaO	0.07	0.07	0.06	0.09	0.06	0.07	0.07
Sum	100.47	100.87	101.20	101.17	100.20	100.39	
—0 for S, F	0.40	0.22	0.37	0.57	0.31	0.35	
Corr. sum	100.1	100.6	100.8	100.6	99.9	100.0	
U (ppm)	408	483	>1000	253	657	268	382
V (ppm)	1277	1210	1346	728	777	678	1002
Köhler—Raaz values							
qz	—11.2	+23.3	—36.0	+35.8	—0.9	+0.6	
F	32.7	39.8	12.9	25.7	40.5	44.7	
fm	56.1	36.9	51.1	38.5	58.6	54.7	

KÅC 1: Uranium-bearing banded meta-tuff. Composed of random samples Kå — 27, 28, 29, 30, 31.
KÅC 2: Uranium-bearing banded meta-tuff. Composed of random samples Kå — 33, 34, 35, 36, 37.
KÅC 3: Uranium-bearing banded meta-tuff. Composed of random samples Kå — 68 A, 68 B. Compare with the modal analysis no. 7 in Table 5.
KÅC 4: Uranium-bearing laminated meta-tuff resembling quartz-biotite schist of Bed 4. Composed of drill-core samples Kå 69001 — 2, 3, 4.
KÅC 5: Uranium-bearing banded meta-tuff. Composed of drill-core samples Kå 69002 — 2, 3, 4, 5.
KÅC 6: Uranium-bearing banded meta-tuff. Composed of drill-core samples Kå 69002 — 6, 7, 8, 9, 10.

TABLE 4b. Chemical analyses of barren banded meta-tuffs from Bed 3

Analysis 001: Sample	3416 KÅC 7	3417 KÅC 8	3418 KÅC 9	3419 KÅC 10	Average
SiO_2	60.6	55.6	54.2	60.1	57.6
TiO_2	0.78	1.0	0.85	0.70	0.83
Al_2O_3	14.6	14.9	15.2	13.8	14.6
Fe_2O_3	1.7	2.2	4.8	1.8	2.6
FeO	5.3	6.2	6.4	6.2	6.0
MnO	0.12	0.15	0.14	0.18	0.14
CaO	3.8	4.7	4.2	4.9	4.4
MgO	4.8	6.3	4.9	4.9	5.2
Na_2O	2.7	1.6	2.4	3.0	2.4
K_2O	2.5	3.7	3.0	2.0	2.8
H_2O >105°	2.1	3.0	2.5	2.0	2.4
H_2O <105°	0.3	0.3	0.6	0.3	0.3
CO_2	0.01	0.01	0.14	0.18	0.08
F	0.12	0.09	0.18	0.10	0.12
S	0.27	0.38	1.3	0.53	0.62
BaO	0.07	0.07	0.06	0.06	0.06
Sum	99.76	100.19	100.87	100.75	
—0 for S, F	0.12	0.13	0.40	0.17	
Corr. sum	99.6	100.0	100.5	100.6	
U (ppm)	< 20	< 20	< 20	< 20	< 20
V (ppm)	376	477	440	263	389
Köhler—Raaz values					
qz	+34.5	+16.9	+14.3	+18.7	
F	30.4	34.3	36.4	35.1	
fm	35.1	48.8	49.3	46.2	

KÅC 7: Barren banded meta-tuff. Composed of random samples Kå — 10, 12, 15.
KÅC 8: Barren banded meta-tuff. Composed of random samples Kå — 55, 211.
KÅC 9: Barren banded meta-tuff. Composed of random samples Kå — 292 A1, 292 A2. Compare with the modal analyses nos. 5 and 4 in Table 5.
KÅC 10: Barren banded meta-tuff. Composed of drill-core samples Kå 69002 — C, D, E.

TABLE 4c. Chemical analysis of the uranium-bearing graphitic meta-tuffite

Analysis 001: Sample	3424 KÅC 11
SiO_2	55.0
TiO_2	0.67
Al_2O_3	12.7
Fe_2O_3	3.0
FeO	7.8
MnO	0.11
CaO	6.8
MgO	6.1
Na_2O	0.8
K_2O	4.0
H_2O >105°	1.7
H_2O <105°	0.2
CO_2	0.08
F	0.15
S	1.9
BaO	0.05
Sum	101.06
—0 for S, F	0.54
Corr. sum	100.5
U (ppm)	382
V (ppm)	1219
C (graphite)	0.16
Köhler—Raaz values	
qz	+21.4
F	26.1
fm	52.5

KÅC 11: Uranium-bearing graphitic meta-tuffite. Composed of drill-core samples Kå 69007 — 1, 2, 3, 4, 6, 7, 8, 9, 10.

TABLE 5. Modal analyses and modal estimates of rocks from the Kopparåsen greenstone belt. In the modal estimates, the following signs have been used: +++ = main minerals; ++ = subordinate minerals; + = accessory minerals

Bed	1		2	3						4		5	14
Analysis	1	2	3	4	5	6	7	8	9	10	11	12	13
Mineral													
Quartz	13	19	12	21	7	18	0.3	0.5	1	50.7	45.0	9.4	2
Albite[1])	+	++	+	27	+	+	—	9	25	6.8	—	—	+
Epidote[2])	65	+++	+++	25	51	42	19.3	12	23	—	—	24.8	—
Aggregate[3])							21.3	12		+	43.3		39
Green biotite	8	+++	++	—	—	—	—	—	—	—	—	—	—
Brown biotite	—	—	—	+	38	26	—	43	44[7])	40.8	10.4	46.8[9])	9
Chlorite[1])	+	+	+	+	+	+	+	18	.[8])	—	—	3.3	+
Muscovite	—	—	—	—	—	13	—	—	—	—	0.8	—	—
Amphibole	14	++	+++	25	2	+	55.5	1	—	—	—	1.1[10])	45
Carbonate	—	—	—	—	—	—	—	—	4	—	—	—	—
Scapolite	—	—	+	+	—	—	—	—	—	—	—	4.6[11])	—
Opaque minerals	+	+	+	0.4	2	2	2.3[5])	3.5	2	1.4	0.1	9.1[12])	5
Accessory	+	+	+	2	+	+	1.3[6])	1	1	0.4	0.3	0.9	
N[4])	1400	700	500	1300	1200	1000	1553	1078	1303	2012	1670	1728	1400

Explanation to Table 5.

1) Relatively large, well individualised grains.
2) Relatively large, often subhedral porphyroblasts.
3) Fine-grained aggregate of albite ± epidote ± chlorite ± mica ± carbonate.
4) Number of points counted.
5) Probably too low as the grains are extremely fine.
6) Included 1 % of sphene.
7) Included phlogopitic mica.
8) As chlorite is fine-grained and forms aggregates with biotite and epidote, it is partly included as aggregate[3]) and partly as biotite.
9) Included also chloritised biotite.
10) Strongly replaced by biotite.
11) Included inclusions in scapolite.
12) Included graphite.

List of analysed rocks in Table 5. Each analysis represents one thin section.

1. Massive meta-tuff, Kå 44—68.
2. Massive meta-tuff, Kå 69002/a.
3. Meta-lava, Kå 64—68.
4. Barren banded meta-tuff. Thin section from the light bed in Fig. 3, Kå 292 A-1.
5. Barren banded meta-tuff. Thin section from the adjacent dark bed in Fig. 3, Kå 292 A-2.
6. Barren muscovite-bearing banded meta-tuff, Kå 12—68.
7. Uranium-bearing banded meta-tuff, Kå 68—68, local block.
8. Uranium-bearing banded meta-tuff, Kå 27—68.
9. Uranium-bearing banded meta-tuff, Kå 36—68.
10. Quartz-biotite schist, type 1., Kå 4—68.
11. Quartz-biotite schist, type 2., Kå 13—68.
12. Uranium-bearing graphitic meta-tuffite, Kå 69007-1.
13. Greenstone, meta-volcanic turbidite, Kå 21—68.

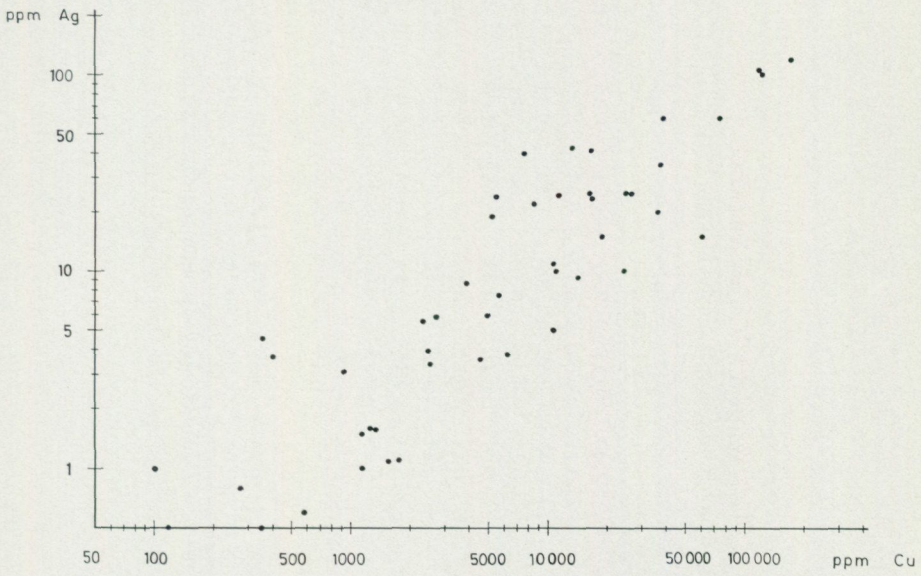

Fig. 42. Correlation of Ag and Cu. Mineral assemblage I, "whole rock" analyses.

TABLE 6a. Mineral assemblage II. — Correlation matrix
The data has been transformed into logarithms

	U	Cu	Pb	Zn	Bi	Ag	Mo	As	Fe_2O_3	TiO_2	CaO	V	Co	Ni
U	1.00	—0.11	0.43	—0.21	0.13	0.13	0.27	0.53	0.26	—0.32	—0.31	0.33	0.21	—0.04
Cu	—0.11	1.00	0.50	0.34	0.16	0.65	—0.18	0.18	0.24	—0.46	0.45	0.65	0.30	0.64
Pb	0.43	0.50	1.00	0.52	0.43	0.85	0.19	0.54	0.63	—0.78	0.32	0.59	0.61	0.55
Zn	—0.21	0.34	0.52	1.00	0.61	0.51	—0.02	—0.24	0.48	—0.52	0.73	0.05	0.45	0.42
Bi	0.13	0.16	0.43	0.61	1.00	0.52	0.51	—0.05	0.68	—0.59	0.63	—0.11	0.48	0.25
Ag	0.13	0.65	0.85	0.51	0.52	1.00	0.36	0.49	0.52	—0.81	0.42	0.50	0.51	0.51
Mo	0.27	—0.18	0.19	—0.02	0.51	0.36	1.00	0.36	0.19	—0.51	0.13	—0.17	0.11	—0.16
As	0.53	0.18	0.54	—0.24	—0.05	0.49	0.36	1.00	0.23	—0.49	—0.29	0.45	0.33	0.19
Fe_2O_3	0.26	0.24	0.63	0.48	0.68	0.52	0.19	0.23	1.00	—0.57	0.40	0.21	0.87	0.58
TiO_2	—0.32	—0.46	—0.78	—0.52	—0.59	—0.81	—0.51	—0.49	—0.57	1.00	—0.55	—0.31	—0.62	—0.45
CaO	—0.31	0.45	0.32	0.73	0.63	0.42	0.13	—0.29	0.40	—0.55	1.00	—0.07	0.39	0.50
V	0.33	0.65	0.59	0.05	—0.11	0.50	—0.17	0.45	0.21	—0.31	—0.07	1.00	0.25	0.28
Co	0.21	0.30	0.61	0.45	0.48	0.51	0.11	0.33	0.87	—0.62	0.39	0.25	1.00	0.67
Ni	—0.04	0.64	0.55	0.42	0.25	0.51	—0.16	0.19	0.58	—0.45	0.50	0.28	0.67	1.00

Number of samples = 23, samples with uranium content >100 ppm U

TABLE 6b. Mineral assemblage III. — Correlation matrix
The data has been transformed into logarithms

	U	Cu	Pb	Zn	Bi	Ag	Mo	As	Fe_2O_3	TiO_2	CaO	V	Co	Ni
U	1.00	0.43	0.86	0.32	0.55	0.76	0.16	0.58	0.44	—0.33	—0.30	—0.18	0.62	0.05
Cu	0.43	1.00	0.65	0.53	0.44	0.80	0.67	0.37	0.94	0.17	0.08	0.20	0.90	0.85
Pb	0.86	0.65	1.00	0.65	0.33	0.87	0.51	0.56	0.71	—0.44	0.03	—0.22	0.74	0.37
Zn	0.32	0.53	0.65	1.00	—0.31	0.43	0.83	0.36	0.73	—0.42	0.65	0.14	0.50	0.56
Bi	0.55	0.44	0.33	—0.31	1.00	0.60	—0.21	0.54	0.21	0.34	—0.78	0.02	0.59	0.04
Ag	0.76	0.80	0.87	0.43	0.60	1.00	0.35	0.53	0.76	—0.22	—0.14	—0.29	0.80	0.46
Mo	0.16	0.67	0.51	0.83	—0.21	0.35	1.00	0.17	0.76	0.05	0.55	0.36	0.61	0.80
As	0.58	0.37	0.56	0.36	0.54	0.53	0.17	1.00	0.33	—0.11	—0.31	0.20	0.65	0.02
Fe_2O_3	0.44	0.94	0.71	0.73	0.21	0.76	0.76	0.33	1.00	—0.04	0.31	0.17	0.84	0.86
TiO_2	—0.33	0.17	—0.44	—0.42	0.34	—0.22	0.05	—0.11	—0.04	1.00	—0.41	0.62	0.20	0.31
CaO	—0.30	0.08	0.03	0.65	—0.78	—0.14	0.55	—0.31	0.31	—0.41	1.00	0.02	—0.17	0.31
V	—0.18	0.20	—0.22	0.14	0.02	—0.29	0.36	0.20	0.17	0.62	0.02	1.00	0.30	0.33
Co	0.62	0.90	0.74	0.50	0.59	0.80	0.61	0.65	0.84	0.20	—0.17	0.30	1.00	0.68
Ni	0.05	0.85	0.37	0.56	0.04	0.46	0.80	0.02	0.86	0.31	0.31	0.33	0.68	1.00

Number of samples = 15, samples with uranium content >100 ppm U

APPENDIX: Phase analyses of the Cu-Fe-S minerals by X-ray diffraction

by

A. M. BYSTRÖM-BRUSEWITZ

In an attempt to better define the digenite, which had been observed under the optical microscope, an X-ray diffraction analysis was performed at the Geochemical Division, SGU. The sample no. Kå-193 was chosen. In this sample, light blue isotropic digenite is intricately intergrown with bornite and magnetite, with the former mineral forming relatively coarse subgraphic textures. A diffractogram of a sample from which the magnetite has been removed shows reflections from bornite and digenite in about equal parts. Some impurities of quartz and feldspar are present. A fraction with nearly pure digenite was obtained by separation in heavy liquids and by the Franz isodynamic magnetic separator. The less magnetic fractions were enriched in digenite. The diffractogram of the powdered sample gave broad, diffuse peaks and it was not possible to obtain precise measurements. However, by warming the specimens for some hours at 140°C, the peaks in the diagram became sharp.

TABLE 7. X-ray diffraction data of bornite-digenite fractions, Cu Kα-radiation, Philips diffractometer

Digenite-bornite				Digenite			
2Θ	$\sin^2\Theta$	hkl	phase	I	2Θ	$\sin^2\Theta$	hkl
27.02	0.05458	6 2 2	B				
27.83	0.05783	5 5 5	D	st	27.89	0.05808	5 5 5
28.24	0.05951	4 4 4	B				
29.34	0.06414	9 1 1	D		29.45	0.06461	9 1 1
31.89	0.07547	6 5 0 6 4 3	B				
32.27	0.07723	10 0 0	D	vst	32.30	0.07737	10 0 0
32.70	0.07924	8 0 0	B				
35.47	0.09279	10 4 2 ?	D				
35.82	0.09457	11 1 1 ? 6 6 2 ?	D B		35.82	0.09457	11 1 1
41.57	0.12593	9 9 1	D		41.75	0.12697	9 9 1
46.22	0.15405	10 10 0	D		46.33	0.15475	10 10 0
46.85	0.15804	8 8 0	B				
54.83	0.21200	15 5 5	D	st	54.86	0.21221	15 5 5
55.67	0.21802	12 4 4	B				
					59.48	0.24608	
					67.50	0.30866	20 0 0

(There is a slight missalignment of the machine at larger angels which has not been considered.) The quartz peak at 26.66° has been used to correct the 2Θ values.

Cell dimensions were calculated. The 1 0 1 quartz peak was used to correct the positions of peaks. From the diffractogram with both phases the following values were obtained:

bornite — 21.91 ±0.04Å with 95% confidence

digenite — 27.76 ±0.05Å with 95% confidence (11 1 1 not included)

A diagram of the purified digenite fraction, also with the quartz peak 1 0 1 as a reference, gave the following value for the large unit cell — 27.72 ±0.04Å — when only indices of multiples of 5 were used. When all indices are included, the unit cell has a value of 27.71 ±0.16Å at 95% confidence. This indicates that the larger cell is not strictly cubic. The figure 43 shows diagrams of the two fractions.

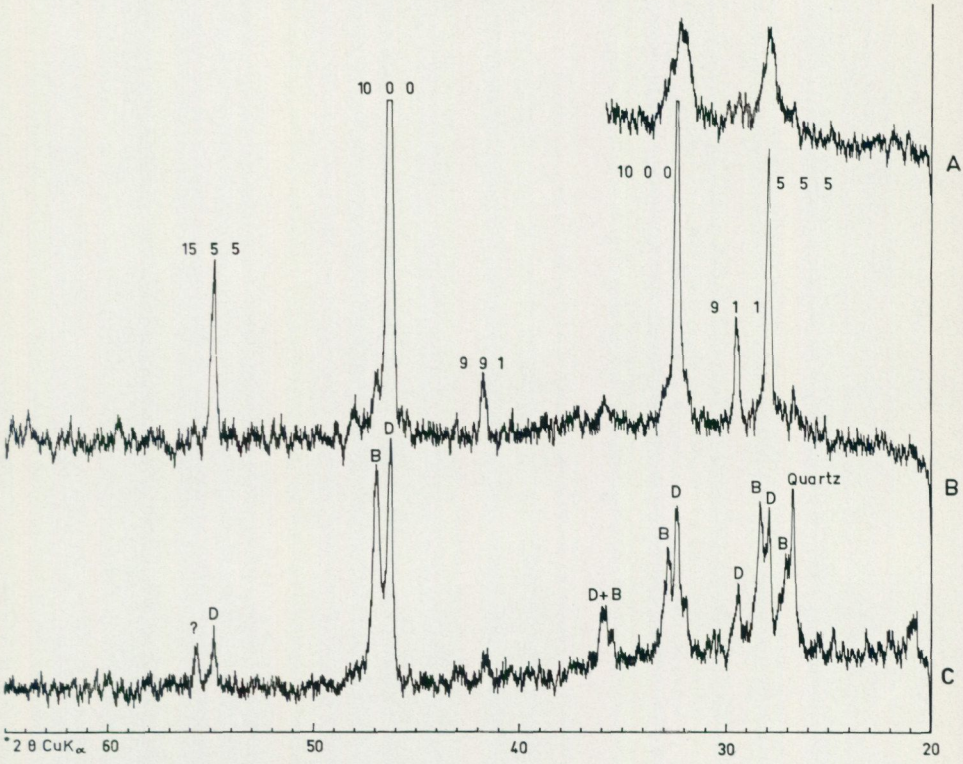

Fig. 43. X-ray diffractograms, powder mounted on glass slide, Cu Kα-radiation.
A. Digenite, ground powder.
B. Digenite, ground powder heated for 2 hrs at 140° C.
C. Digenite + bornite, ground powder heated for 2 hrs at 140° C.

GEOLOGICAL MAP
OF THE
KOPPARÅSEN GREENSTONE BELT

Pavel Adamek 1975

Scale 1:20000

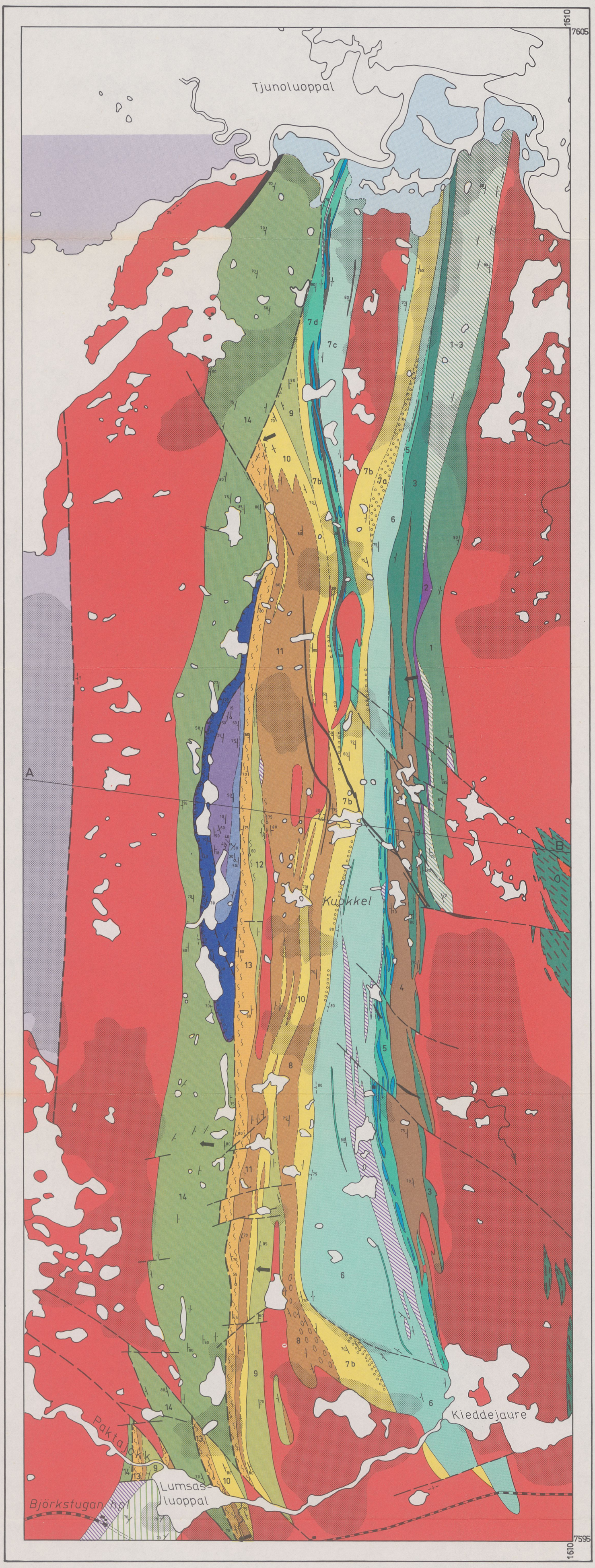

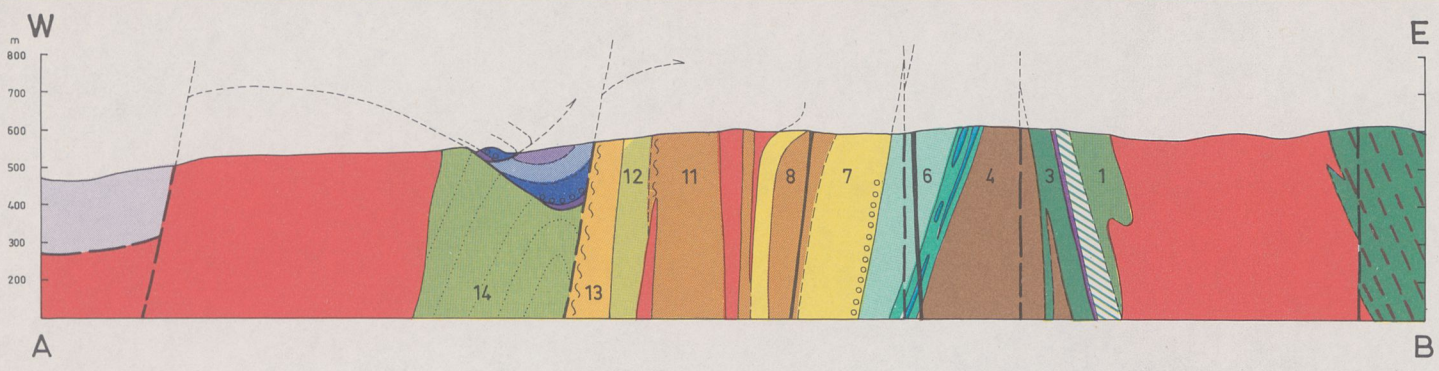

LEGEND

Alluvium

TORNETRÄSK GROUP

Shale

Sandstone with interlayered thin beds of shale

Quartzitic sandstone with basal conglomerate

Basal shale

Undifferentiated Caledonian rocks

Dolerite dykes

Migmatite-granite

KUOKKEL GROUP

14 Greenschist

Meta-porphyrite sills

13 Strongly sheared sandstone and pebbly sandstone

12 Greenschist

11 Pebbly sandstone

10 Sandstone and quartzite

9 Greenschist

8 Pebbly sandstone

Conglomerate

7b Sandstone and quartzite

7a Conglomerate

6,7c Meta-volcaniclastic psephite (pyroclastic breccia, lapilli-tuff, sharpstone conglomerate) with associated meta-tuff

Graphite-bearing meta-tuffite

5,7d Meta-tuff, graphite-bearing meta-tuffite, meta-cherty tuff

Graphite schist

Meta-chert

4 Quartz-biotite schist

3 Banded meta-tuff

Greenschist (transitional rocks between Bed 1 and Bed 3)

2 Meta-basic lava

1 Massive meta-tuff

Undifferentiated greenstones of uncertain stratigraphic position

Migmatised greenstones

Areas mostly covered by glacial drift

Lithologic boundary, sharp
,, ,, , successive

70 Bedding

Way up determination

20 Cleavage

Minute fold axis

Fault

Reverse fault

Thrust

Shear zone

RADIOACTIVE ANOMALIES OF THE KOPPARÅSEN GREENSTONE BELT

Pavel Adamek 1975

Scale 1:20000

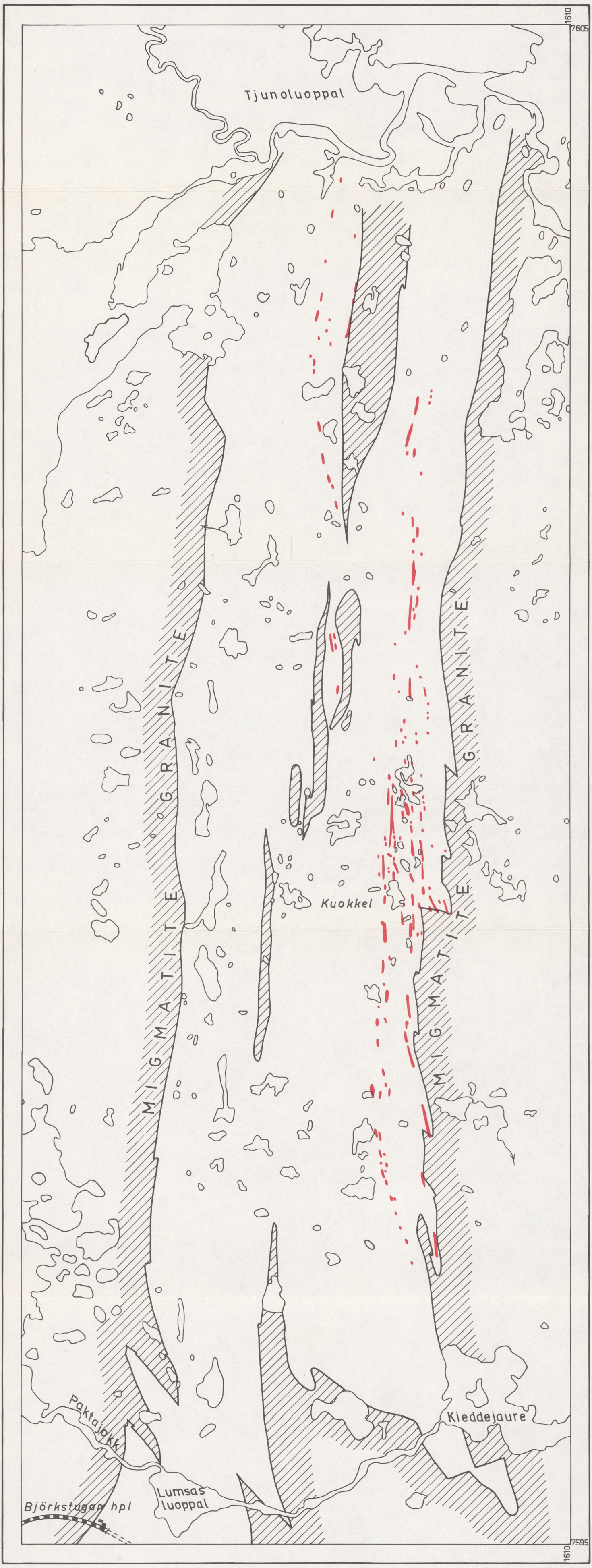

Semisystematic ground measurements. Instrument: Scintillometer NE 148 A (Yellow box)

Radioactive anomalies > 100 μ R/h

INDEX MAP SHOWING THE LOCATION OF ORE MINERALS IN THE KOPPARÅSEN GREENSTONE BELT

Pavel Adamek 1975

Scale 1:20000

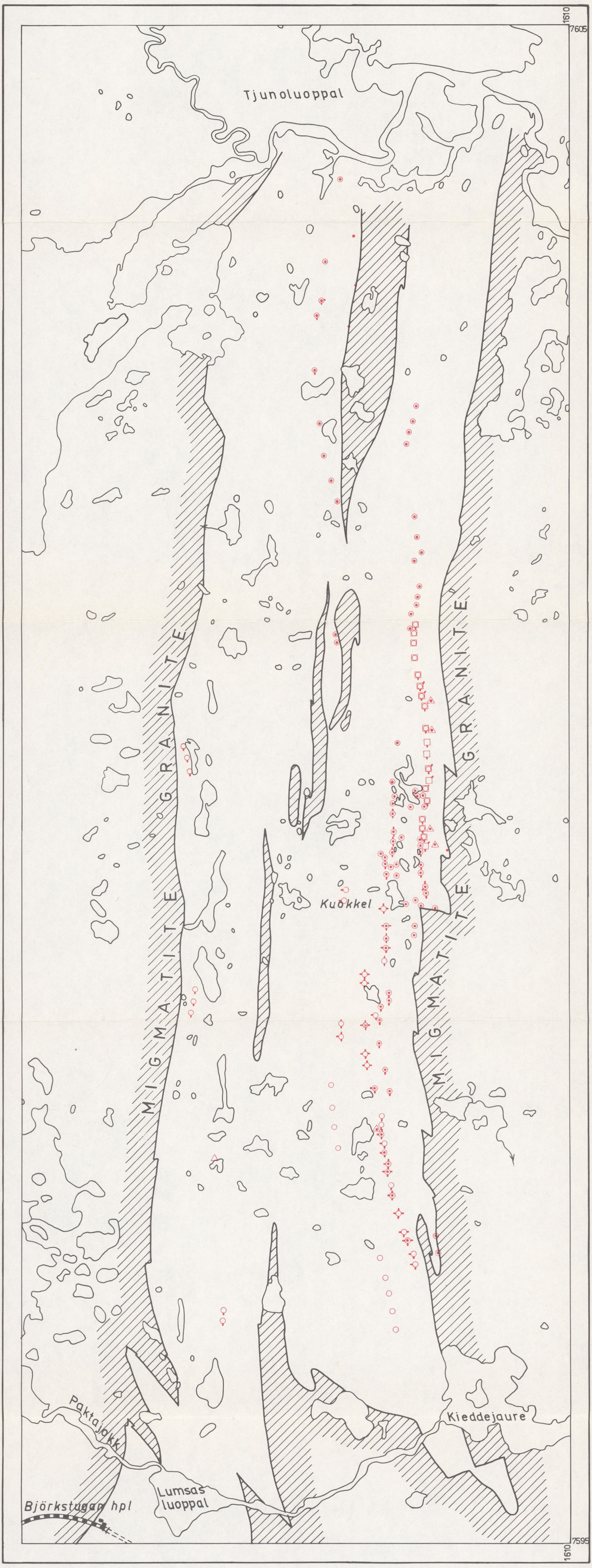

LEGEND

- Magnetite (Mg)
- (Mg) + pyrite
- (Mg) + bornite + digenite
- (Mg) + chalcopyrite
- Uraninite
- Pyrite (Py) ± pyrrhotite (Po)
- (Py ± Po) + arsenopyrite
- (Py ± Po) + chalcopyrite
- (Py ± Po) + sphalerite
- (Py ± Po) + galena
- (Py ± Po) + molybdenite
- (Py ± Po) + gersdorffite
- Skarn or skarn-like bodies

GEOLOGICAL MAP OF THE AREA 70–340 m SOUTH OF THE KUOKKEL CABIN

Pavel Adamek **1975**

Scale 1:400

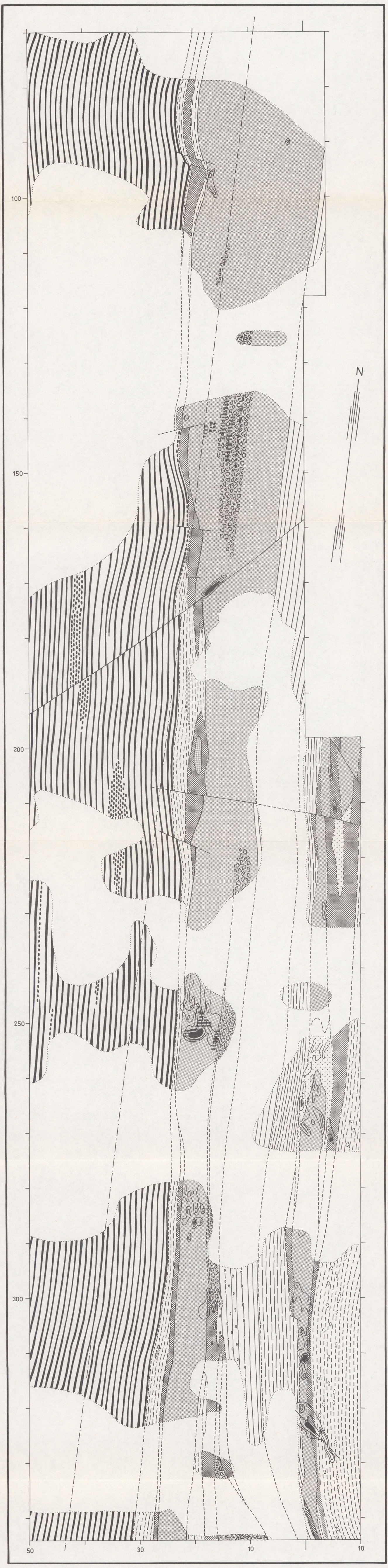

LEGEND

Bed 6

- Layered meta-tuff associated with meta-pyroclastic breccia
- Layered meta-tuff with transitions to fragment-bearing meta-tuff
- Layered or massive meta-tuff
- Skarn-like mobilisates

Bed 5

- Graphite-bearing meta-tuffite with minute lenticles of chert
- Graphite-bearing meta-tuffite rich in sulphide minerales
- Banded or massive chert
- Chert of breccia structure
- Chert rich in sulphide minerals

Radioactive anomalies with isolines of:

- 30 μR/h
- 100 μR/h
- 300 μR/h

PRISKLASS H

Distribueras genom
LiberTryck
162 89 VÄLLINGBY

Växjö 1975, C. Davidsons Boktryckeri AB
Printed in Sweden

ISBN 91-7158-076-X